2011

Performance Analysis of Modern Communication System in Realistic Environment

Jamil Hussain

Performance Analysis of Modern Communication System in Realistic Environment

(Spine title: Perf. Analysis of Modern Comm. System in Realistic Environment)

(Thesis format: Monograph Article)

by

Jamil Hussain

Graduate Program
in
Engineering Science
Electrical and Computer Engineering

A thesis submitted in partial fulfillment
of the requirements for the degree of
Master of Engineering Science

School of Graduate and Postdoctoral Studies
The University of Western Ontario
London, Ontario, Canada

Certificate of Examination

THE UNIVERSITY OF WESTERN ONTARIO
SCHOOL OF GRADUATE AND POSTDOCTORAL STUDIES
CERTIFICATE OF EXAMINATION

Chief Advisor:

Dr. Serguei Primak

Advisory Committee:

Examining Board:

Dr. Raveendra Rao

Dr. Quazi Rahman

Dr. Liying Jiang

The thesis by
Jamil Hussain
entitled:
Performance Analysis of Modern Communication System in Realistic Environment
is accepted in partial fulfillment of the
requirements for the degree of
Master of Engineering Science

Date: _____

Chair of Examining Board
Dr. James Lacefield

Abstract

Multiple Input Multiple Output (MIMO) technique is one of the effective techniques to combat against fading in wireless communication system. In this thesis, based upon that, performance is evaluated for MIMO system while considering some practical scenario which was ignored for simplicity in previous works. Apart from that it is well known now a days that co-operative communication has created a new class of communication technique in wireless communication arena. It is also investigated in this thesis work how the system performs while implementing co-operative communication system in an industrial application where the environment is much different from the traditional environment due to the presence of Impulse Noise. Later co-operative communication system and the diversity technique are blended together and the performance of such system is analyzed theoretically as well as in simulation. Results acquired in this thesis will be used to bring forth publication.

Key Words : *MIMO, Alamouti Code, Angle of arrival, Doppler spread, Probability of Error, Co-operative Communication, Physical Network Coding, Impulse Noise, Bi-directional Relay Network, Co-operative Diversity.*

Acknowledgements

It is my pleasure to write down about the people who helped me, gave me courage to pursue my graduate studies in The University of Western Ontario. At first I would like to express my gratitude and appreciation to my supervisor, Dr. Serguei Primak who has been of great help to accomplish this thesis. His way of sensible guiding, wisdom and overall being as a perfect mentor helped me to reach my goal in a short time. Certainly it has been rewarding to get him as my supervisor. I also would like to thank to the committee members in my thesis defence. Their valuable suggestions, constructive comments and reviews made my whole work more worthy.

I also would like to thank my parents, family members who always supported and encouraged me for everything I achieved throughout my life. Their contributions were a big catalyst to reach to my target. My special gratitude will go to my friends in overseas whose presence, support and prayer boosted me in every bit of my life here. I was fortunate to have some good colleagues in my lab to work with. Finally I would like to thank Tim Hortons Inc. for their wonderful beverages which always stimulated me to work.

Table of Contents

List of Tables

List of Figures

Acronyms

AOA	*Angle of Arrival*
ANC	*Analog Network Coding*
AF	*Amplify and Forward*
AWGN	*Additive White Gaussian Noise*
BC	*Broadcast*
BER	*Bit Error Rate*
BPSK	*Binary Phase Shift Keying*
CDF	*Cumulative Distribution Function*
CDMA	*Code Division Multiple Access*
CSI	*Channel State Information*
DF	*Decode and Forward*
DS-CDMA	*Direct Sequence Code Division Multiple Access*
IN	*Impulse Noise*
LHP	*Left Half Plane*
LC-STD	*Low Complexity Space Time Decoder*
MAC	*Multiple Access*
MIMO	*Multiple Input Multiple Output*
ML	*Maximum Likelihood*
ML-STD	*Maximum Likelihood-Space Time Decoder*
PDF	*Probability Density Function*
PNC	*Physical-layer Network Coding*
PSD	*Power Spectral Density*
RHP	*Right Half Plane*
Rx	*Receive Antenna*
SEP	*Symbol Error Probability*
SIR	*Signal to Impulse noise Ratio*

SISO	*Single Input Single Output*
SNR	*Signal to Noise Ratio*
STBC	*Space Time Block Code*
STD	*Space Time Decoder*
STTD	*Space Time Transmit Diversity*
Tx	*Transmit Antenna*

Chapter 1
Introduction

Demands in wireless communication are increasing day by day as the technology in this sector is flourishing tremendously. The system has to have high voice quality, high data rate, good coverage area, high power and bandwidth efficiency and be cost effective. In order to meet those requirements different technologies are proposed in years and still researchers are devoted to invent new ones. While fulfilling one demand, in almost every case, another parameter is to be sacrificed. In some cases, reasonable trade off can be done to meet specific requirements. Theoretically the main objective of wireless communication is not to lose any benefit to achieve another. However due to several limitations it may not be possible to do that practically. Hence designing of a system must be done in such a manner that the sacrifice in other parameters is least.

The fundamental phenomenon which makes wireless communication difficult is multipath fading [1]. To combat against multipath fading, numerous techniques have been developed. One of the most efficient ways to mitigate multipath fading is by using diversity technique. The key idea of diversity technique is to create several replica of the transmitting signal at the reception side. Proper combination of those replicas can reduce the effect of multipath fading and hence improve the reliability of the transmission. Of different types of diversity techniques, space diversity is to be considered for this thesis work. Alamouti's [2] diversity technique was a significant work in the arena of diversity techniques. There were some assumptions in that work

to make the whole system simple to analyse. For example it was assumed that channel will not vary in two consecutive time cycle and the channel condition is perfectly known at the receiver. In real case those situations might not be possible. There is less possibility that channel will remain fixed in exactly two consecutive time sequence. To determine the channel condition pilot symbols are normally inserted with original information. Pilot symbols can not always determine the channel condition perfectly. It can happen in two cases. First, when the pilot symbols are not received at the reception side perfectly. Secondly when the channel fades too quickly with time. Pilot symbols are normally inserted after a fixed time period. If the channel fades fast, it is not possible to determine the Channel State Information (CSI) perfectly. In this thesis, performance is evaluated when the channel condition changes in every time symbol. It is also considered that the pilot symbols might be erroneous and the channel might change fast. Those analysis are shown in Chapter 3. Theoretical as well as simulated results are presented to investigate such condition.

Although diversity techniques offer various advantages, it may not always be possible to deploy multiple antennas due to the hardware complexity, size and power of the terminal. In such scenarios, alternative measures should be taken to mitigate the effect of noise at the reception end. Co-operative communication is then attracted by the researchers to combat against those shortcomings. It is indeed a promising topic in the most recent years due to its extended coverage area, overall capacity and enhanced reliability [3]. Extensive researches are going on to utilize the benefits offered by this technology. Apart from those points mentioned, co-operative communication can also be considered as an effective means of communication where it may not be possible to transmit signal from transmitter to receiver due to the long distance or placement of terrain contours like hills, tall buildings *etc.* between transmitter and receiver. A relay node is placed between transmitter and receiver which retransmits the received

signal from transmission end. Hence it can increase the coverage area of the whole system. In addition noise makes wireless reception vulnerable. Since an extra node is used between the transmitter and the receiver, that node processes and intensifies the signal strength which makes the transmitted signal to be less prone to system noise. These things are discussed elaborately at the beginning of Chapter 4. Then a new factor is considered for wireless communication for an industrial environment. Apart from traditional communication system there is one extra factor which has great impact on the overall performance and that is Impulse Noise. It is not possible to define impulsive nature of environment with conventional Additive White Gaussian Noise (AWGN) model. In an industrial environment there are numerous sources of impulse noise like in electro-mechanical devices, automobiles, ignition system, high power elements *etc* [4]. Those sources create spikes at the reception side of the system which can make it difficult to detect the required signal. Performances are analysed while varying the frequency of occurrence of the impulse noise in Chapter 4.

Another important and promising sector of wireless communication is analysed in the later part of Chapter 4 and it is co-operative communication with diversity technique. Co-operative communication system and diversity technique have their own several advantages. If they can be combined with each other, it would be possible to reap the advantages of both techniques. It would also be possible to enhance transmission quality and optimize power allocation of the whole system [5]. Theoretically the performance of such system is discussed in details in Chapter 4. The upper limit and the lower limit of the system performance will be derived. Simultaneously, performance will also be evaluated by simulating the system implementing both techniques. Apart from Chapter 3 and Chapter 4, it is tried to give a basic technical idea on different topics aimed for this thesis in Chapter 2 while Chapter 5 will yield conclusion of the thesis.

The contribution of this thesis can be described in three steps. At first, analysis of Alamouti's Scheme while considering that pilot symbols are to be erroneous and channel changes fast in a non-isotropic environment. Later, system performance of a wireless system is analysed for an industrial environment where impulse noise becomes a significant factor. Then last but not the least, co-operative communication has been merged with diversity technique with theoretical analysis as well as simulation.

Chapter 2

Background

The objective of this chapter is to provide technical background on selected topics on wireless communication relevant to this research study. At first explanation will be given to some basic terms which are utilized in later chapters. Basic ideas will also be given for MIMO communication system including Alamouti's Space Time Coding. Finally there will be discussion on a new area of communication system, namely, co-operative communication system.

2.1 Some definition(s)

In this section, definition will be given on some topics which will then be used throughout the whole work.

2.1.1 Cumulative Distribution Function

In probability theory, Cumulative Distribution Function (CDF) describes the probability of a random variable X to be found less than or equal to a specific value x. So CDF of a real-valued random variable can be defined as [6]

$$F(x) = P(X \leq x) \tag{2.1}$$

for every x from $-\infty$ to $+\infty$.

The Cumulative Distribution Function, $F(x)$ has the following properties [7]:

1. $F(x)$ is a non-decreasing function. It means if $x_1 < x_2$, then $F(x_1) < F(x_2)$. Hence $F(x)$ can increase or stay at the same level. However it can never decrease.

2. $0 \leq F(x) \leq 1$

3. $\lim_{x \to \infty} F(x) = F(\infty) = 1$

4. $\lim_{x \to -\infty} F(x) = F(-\infty) = 0$

It will be shown later that if Cumulative Distribution Function is known, Probability Density Function can be calculated and vice-versa.

2.1.2 Probability Density Function

Discrete random numbers have a finite number of values or countably infinite number of values. There also exists another group of random numbers which have infinite number of values or uncountable set of values. Those are called continuous random numbers. Therefore a random number is said to be continuous if there exists a function $f(x)$ where $-\infty \leq x \leq \infty$ which has the property

$$P(X \in A) = \int_A F(x)dx \tag{2.2}$$

The function $f(x)$ is called Probability Density Function (PDF) and can be defined as [7]:

$$f(x) = \frac{dF(x)}{d(x)} \tag{2.3}$$

The Probability Density Function (PDF) has following properties [8]:

1. $f(x) \geq 0$
2. $\int_{-\infty}^{\infty} f(x)dx = 1$
3. $P(a \leq X \leq b) = \int_{a}^{b} f(x)dx$ There is relationship between PDF and CDF.

Depending upon the situation problems can be solved either by calculating CDF or PDF [9].

2.1.3 Q-function

Q-function or $Q(x)$ is the probability of a standard normal random variable will have a value larger than x. It can be expressed as

$$Q(x) = \frac{1}{\sqrt{2\pi}} \int_{x}^{\infty} \exp\left(\frac{-t^2}{2}\right) \tag{2.4}$$

$Q(x)$ function has a property of [7]

$$Q(-x) = 1 - Q(x) \tag{2.5}$$

In communication system, $Q(x)$ plays an important role. It is basically used frequently to derive the error probability of a system.

2.1.4 Fading

Fading is one of the biggest challenges in wireless communication system. Unlike the wired channel which is easy to predict and model, wireless channel is too much difficult to estimate for its extreme randomness [10]. When a signal is propagating

from transmitter to receiver, objects between them might absorb, reflect, diffract or scatter the signal. Due to these factors, the signal is transmitted to the receiver over different paths. Since the travelling paths are not of equal distance, the signals arrive at the receiver after different time delays. When receiver adds those signals together to retrieve the original signal, the amplitude and phase of the received signal gets changed. This phenomenon is called fading [11]. Due to fading the information sent from the transmitter to receiver gets changed and hence makes the situation difficult for the reception end to retrieve the original one.

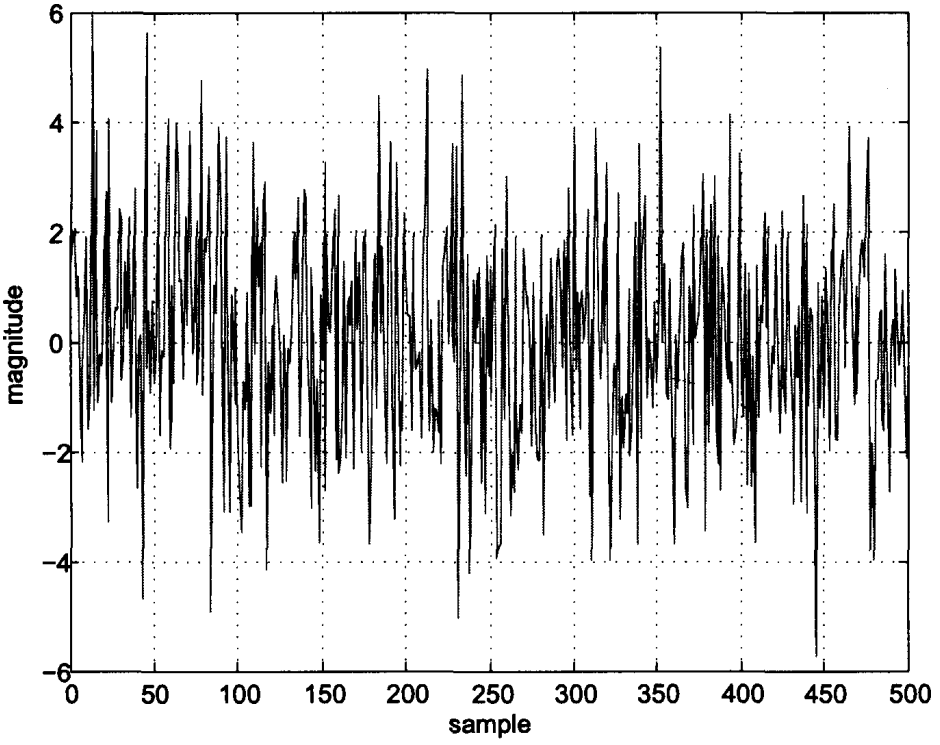

Figure 2.1: Typical Fading Diagram

Figure-2.1 shows a typical diagram of a fading channel. It shows how frequently the magnitude of the channel condition is varying.

2.1.5 Diversity Technique

Diversity technique has been using for years to combat against the multi-path fading in wireless communication system. The basic idea of diversity technique is to send several copies of information signal over different time, frequency or space to the receiver. So there will be least probability that each replica will experience deep fading simultaneously [12]. The objective is that at least one of the replicas will be received correctly and hence the system will not be in outage. Diversity can also be defined quantitatively. If γ represents received signal's SNR and P_e be the probability of error, then the diversity or the diversity gain can be expressed as [12]

$$G_d = -\frac{\log(P_e)}{\log \gamma} \tag{2.6}$$

There are several methods to achieve diversity in a wireless communication system. Those are

1. Temporal or Time Diversity
2. Frequency Diversity
3. Space Diversity

2.1.5.1 Temporal or Time Diversity

In time diversity, the signal is transmitted several times at different time intervals. Certainly the separation of the time intervals has to be sufficiently large. It should be more than the coherence time of the channel [13] as shown in figure-2.2. Coherence time is the time duration over which the impulse response of the channel does not change. In such case, it can be assured that the interleaved symbol is independent

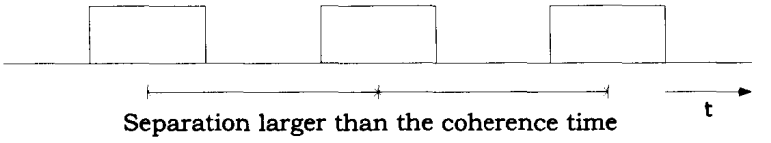

Figure 2.2: Time Diversity Scheme

of previous symbol and hence the diversity can be attained. However for quasi-static channel, the fading is too slow that the channel encountered remains the same regardless of how long it is waited to transmit replicas [14]. The channel remains the same which consequently means that no diversity can be achieved.

2.1.5.2 Frequency Diversity

Frequency diversity can be realized by transmitting different replicas of the information signal over different carrier frequency bands. To achieve the diversity, carrier frequencies should be separated by more than the coherence bandwidth of the channel [12] as shown in figure-2.3. It should be mentioned here that coherence bandwidth implies the range of frequencies over which the channel remains flat. For example, if

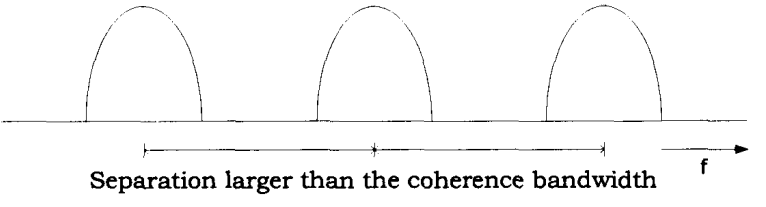

Figure 2.3: Frequency Diversity Scheme

the multipath spread of the channel is $200\mu s$, it implies that a minimum of 5kHz frequency separation is required to achieve the diversity. One drawback of this strategy is that it requires more bandwidth for attaining diversity.

2.1.5.3 Space Diversity

Space diversity is also called antenna diversity. Multiple antennas are used at transmitter or receiver end to achieve the diversity. Different replicas of the information signal will then be received separately by the receiver as illustrated in figure-2.4. If

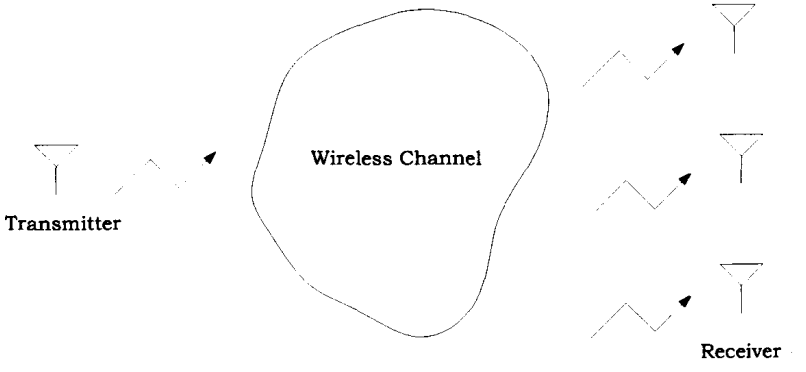

Figure 2.4: Spatial Diversity Scheme

the antennas are separated enough from each other, more than the half of the wavelength, then the received signal will experience different fading hence providing the diversity.

2.1.6 Impulse Noise

Impulse Noise is normally discussed in wireline communication system. Basically it is generated in the switching devices used in that type of communication system. However recent studies has shown that it has effect on wireless communication system in industrial applications. In different kind of industries high voltage devices, automobiles, fluorescent tubes, ignition from mechanical equipments *etc.* create impulse noise which have effect on the wireless communication system.

Impulse Noise is such a noise which creates some unwanted spikes after some intervals depending upon the severity of the noise condition. The simplistic way

to represent impulse noise is by Bernoulli-Gaussian model [15]. Bernoulli-Gaussian process is just simple multiplication of Bernoulli process and Gaussian process as follows

$$i_k = b_k g_k \tag{2.7}$$

Here i_k is the impulse noise, b_k is Bernoulli's process and g_k is Gaussian process with zero mean. Bernoulli's process is a sequence of ones and zeroes with probability p that b_k is one.

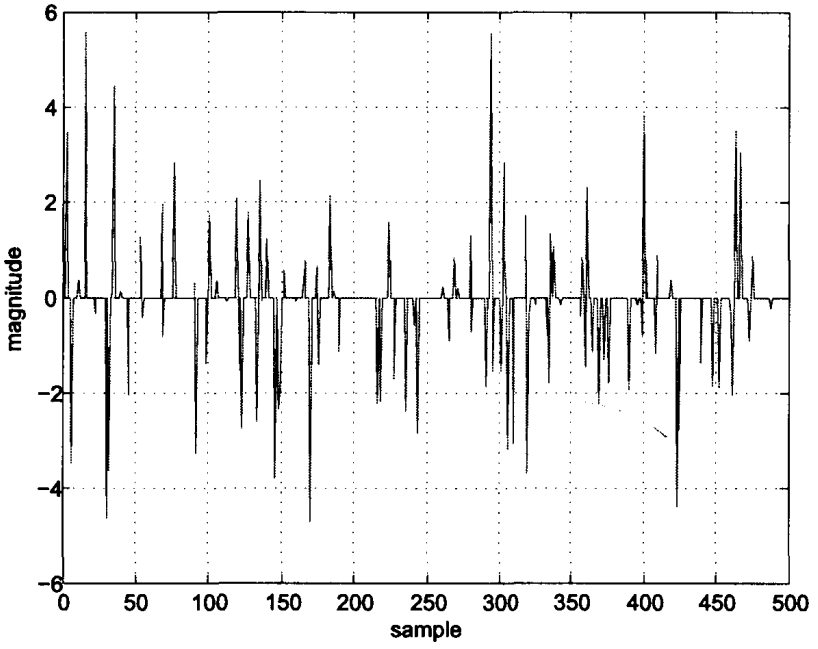

Figure 2.5: Impulse noise with p=0.2

Figure-2.5 shows a typical diagram of impulse noise when probability of occurrence of 1 is 0.2 and figure-2.6 shows the impulse noise with probability of occurrence of 1 is 0.6.

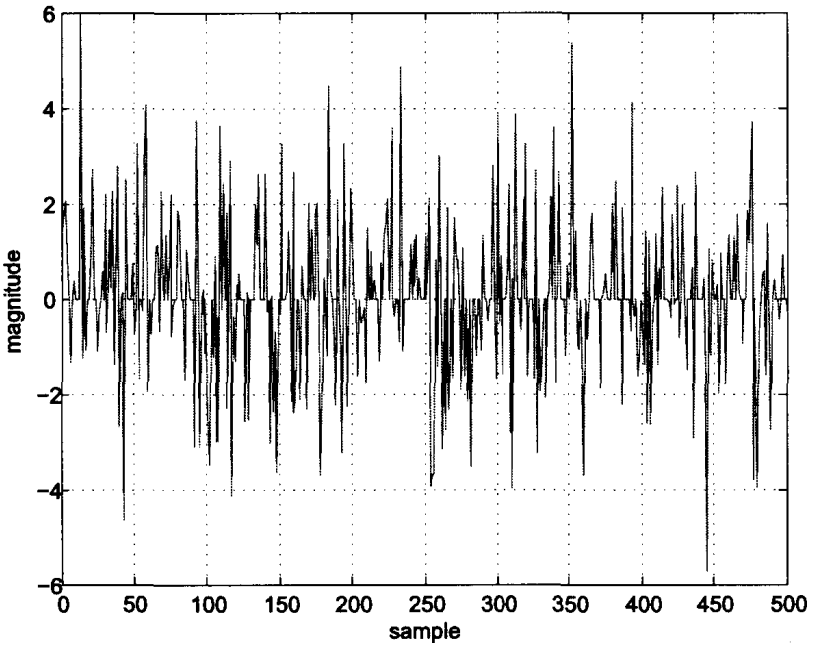

Figure 2.6: Impulse noise with p=0.6

2.2 Alamouti's Scheme

The demand in wireless communication system is simple as to have better performance, power and bandwidth efficiency and the capability to sustain in a diverse environment [2]. Diversity techniques are widely been used to effectively reduce the effect of multipath fading and to improve the reliability of transmission without sacrificing the bandwidth as well as the transmission power [16] [10]. Alamouti suggested a low complex linear combining scheme which is able to completely remove the effect of interference under the assumption of perfect channel estimation as well as quasi-static channel [17]. The key feature of Alamouti's scheme is that it achieves full diversity gain using Maximum Likelihood decoding algorithm [18].

The modulation scheme that had been considered for Alamouti's scheme is BPSK. After modulation the bits are coded and then transmitted through the transmit antennas. The coding and the transmission is done in such format that the data rate does not change from the conventional system. There are two schemes proposed

by Alamouti. Those are:

1. Tx = 2, Rx =1
2. Tx = 2, Rx =2

2.2.1 Alamouti's Scheme with Tx=2, Rx=1

Two transmit antennas and one receive antenna are used here which is shown the figure-2.7.

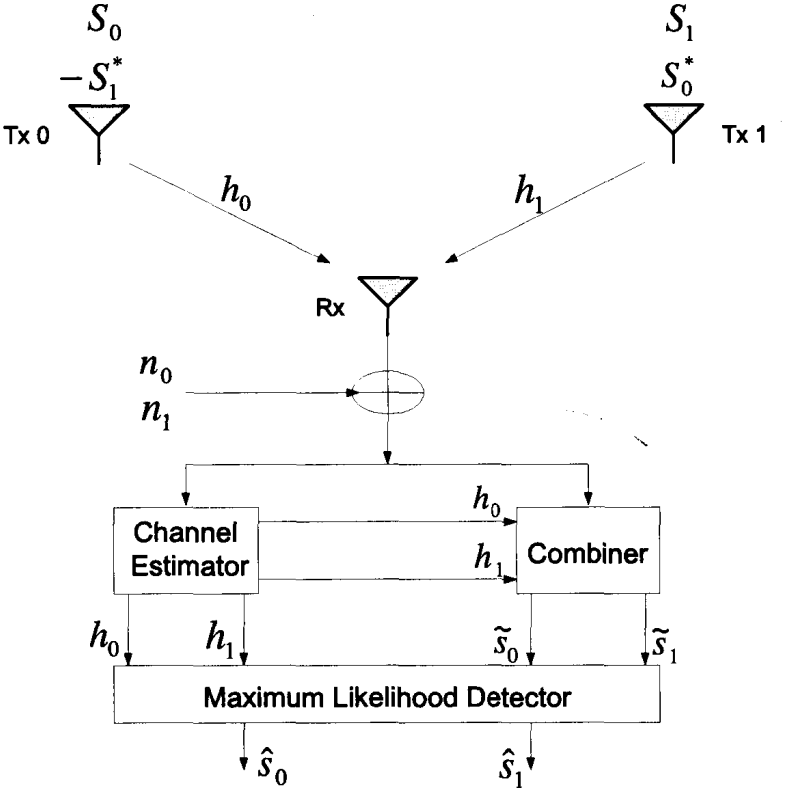

Figure 2.7: Alamouti's Diversity Scheme with Tx=2, Rx=1

At a given time cycle, two signals are transmitted simultaneously from two transmitters. At first time cycle, antenna zero will transmit s_0 and antenna one will transmit s_1. During second time cycle, $-s_1^*$ will be transmitted from antenna zero and s_0^* will be transmitted from antenna one. The sequence is shown in table-2.1.

Table 2.1: Transmission Sequence of Alamouti's Scheme (Tx=2, Rx=1)

Symbol Time	Antenna 1	Antenna 2
1	s_0	s_1
2	$-s_1^*$	s_0^*

The channel co-efficient from first antenna is denoted by $h_0(t)$ and from second antenna is $h_1(t)$. It is assumed that channel co-efficient remains constant during two consecutive bit transmission time. It can be expressed as follows

$$\begin{aligned} h_0(t) &= h_0(t+T) = h_0 \\ h_1(t) &= h_1(t+T) = h_1 \end{aligned} \tag{2.8}$$

The received signal can be expressed as,

$$\begin{aligned} r_0 &= r(t) = h_0 s_0 + h_1 s_1 + n_0 \\ r_1 &= r(t+T) = -h_0 s_1^* + h_1 s_0^* + n_1 \end{aligned} \tag{2.9}$$

Here r_0 and r_1 are the received signal at time t and $(t+T)$ respectively and n_0 and n_1 are the corresponding received noise and interference.

The beauty of Alamouti's scheme is the combining scheme. The received signal is combined in such a manner that received signal does not have any impact from another signal during two time cycles. The combining scheme is described as,

$$\begin{aligned} \tilde{s}_0 &= h_0^* r_0 + h_1 r_1^* \\ \tilde{s}_1 &= h_1^* r_0 - h_0 r_1^* \end{aligned} \tag{2.10}$$

Putting the values of r_0 and r_1 in the above equation will yield

$$\tilde{s}_0 = s_0(h_0^2 + h_1^2) + h_0^* n_0 + h_1 n_1^*$$
$$\tilde{s}_1 = s_1(h_0^2 + h_1^2) + h_1^* n_0 - h_0 n_1^* \tag{2.11}$$

The derivations are elaborated in Appendix-A.1. These combined signals are then sent to the Maximum Likelihood detector which eventually determines the original bits.

2.2.2 Alamouti's Scheme with Tx=2, Rx=2

Figure-2.8 shows the combinations of two transmit antennas and two receive antennas.

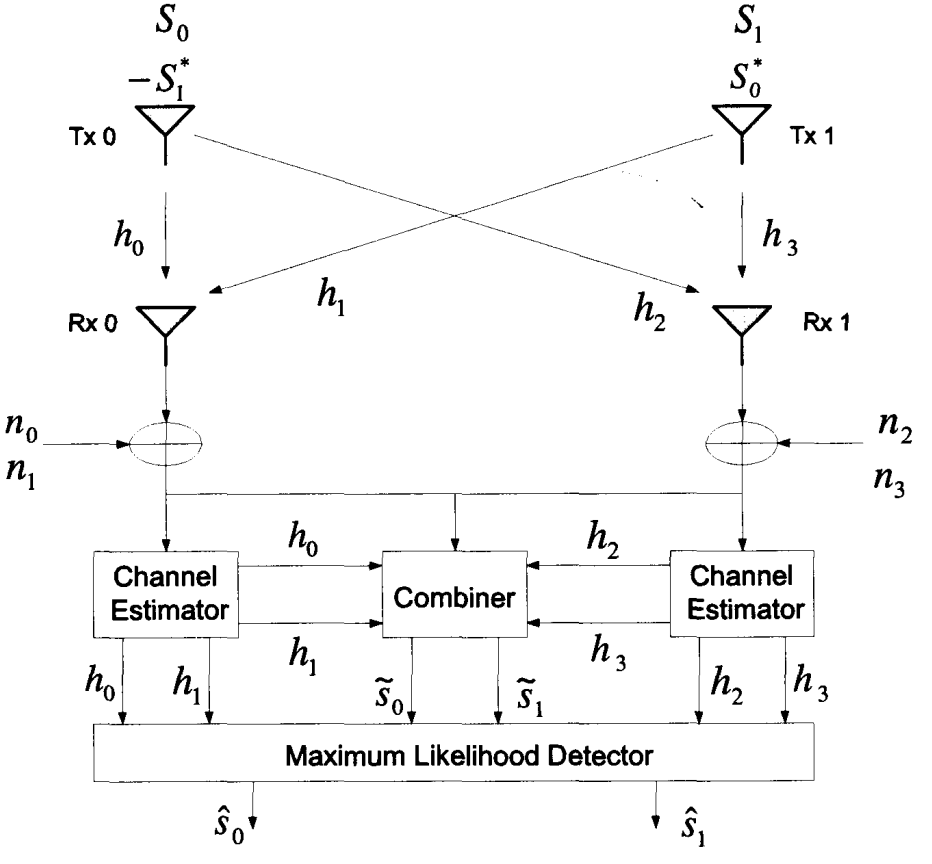

Figure 2.8: Alamouti's Diversity Scheme with Tx=2, Rx=1

Transmission sequence remains the same as the previous case. However, number of channel will increase since number of receive antenna is increased. Table-2.2 describes the channels between the transmit antennas and receive antennas while table-2.3 defines the received signal at different receive antennas.

Table 2.2: Transmission Sequence of Alamouti's Scheme (Tx=2, Rx=2)

	Rx Antenna 0	Rx Antenna 1
Tx Antenna 0	s_0	s_1
Tx Antenna 1	$-s_1^*$	s_0^*

Table 2.3: Received Signal Notation at the receivers (Tx=2, Rx=2)

	Rx Antenna 0	Rx Antenna 1
Time t	r_0	r_2
Time $t+T$	r_1	r_3

The received signal can be represented as,

$$\begin{aligned} r_0 &= h_0 s_0 + h_1 s_1 + n_0 \\ r_1 &= -h_0 s_1^* + h_1 s_0^* + n_1 \\ r_2 &= h_2 s_0 + h_3 s_1 + n_2 \\ r_3 &= -h_2 s_1^* + h_3 s_0^* + n_3 \end{aligned} \tag{2.12}$$

where n_0 , n_1, n_2 and n_3 are the received noises and interferences.

The Combining scheme will be,

$$\begin{aligned} \tilde{s}_0 &= h_0^* r_0 + h_1 r_1^* + h_2^* r_2 + h_3 r_3^* \\ \tilde{s}_1 &= h_1^* r_0 - h_0 r_1^* + h_3^* r_2 - h_2 r_3^* \end{aligned} \tag{2.13}$$

Putting the values in the above two equation will yield (detailed derivation is at Appendix-A.2)

$$\tilde{s}_0 = s_0(h_0^2 + h_1^2 + h_2^2 + h_3^2) + h_0^* n_0 + h_1 n_1^* + h_2^* n_2 + h_3 n_3^*$$
$$\tilde{s}_1 = s_1(h_0^2 + h_1^2 + h_2^2 + h_3^2) + h_1^* n_0 - h_0 n_1^* + h_3^* n_2 - h_2 n_3^* \quad (2.14)$$

Like the previous case, from these two received signals the Maximum Likelihood detector retrieves the original

2.2.3 Simulation and Result

The simulation is done for the typical BPSK system under uncorrelated Rayleigh fading condition using the simulation software Matlab. It is assumed that the total transmit power remains the same for every combination. It has also been assumed that the receivers have the perfect knowledge of the channel condition. The BER performance curves for different combinations are shown in figure-2.9.

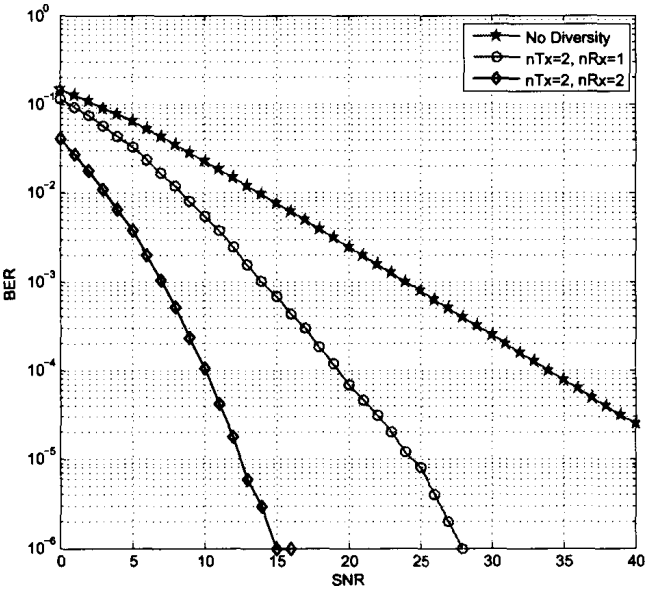

Figure 2.9: Performance comparison among different schemes using Alamouti's Technique

In the figure, curve with star pointer represents the performance curve when no diversity technique is used which means only single transmit antenna and single receive antenna is used. When two transmit antenna and one receive antenna are used, the curve with circle pointer is attained as BER performance. It shows that at least 10 dB performance improvement can be gained when Bit Error Rate is 10^{-3}. The last curve is the performance curve when two transmit antennas and two receive antennas are used. It shows that it can further improve the performance compared to the scheme using two transmit antennas and one receive antennas. The performance gain is around 7 dB at 10^{-3} BER.

2.3 Co-operative Communication System

Co-operative communication has recently drawn tremendous attention to the research community. It is a new communication paradigm which generates independent paths between the user and the base station by introducing a relay channel [3]. In this section, the objective is to provide a basic idea on Co-operative Communication System in brief.

Depending upon the situation and requirements, different protocols are used in co-operative communication system namely Amplify and Forward, Decode and Forward also known as Physical Network Coding (PNC) etc. In Amplify and Forward scheme, the relay simply receives the information signal from the source and amplifies the signal and then retransmits to the destination node while in Decode and Forward scheme, the relay node decodes the signal partially or fully and then retransmits it to the destination node.

Let us consider three node linear wireless network shown in figure-2.10. Here node-1 and node-3 exchange information with each other while node-2 is the relay

node.

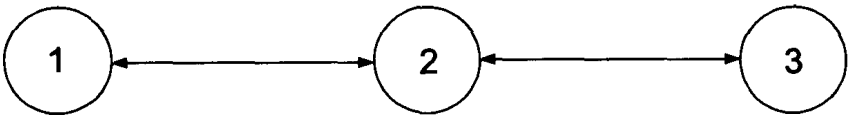

Figure 2.10: A three node wireless network

There are several methods for the information to be transmitted from the source to the destination based on the number of time slots. A traditional transmission schedule is given in figure-2.11.

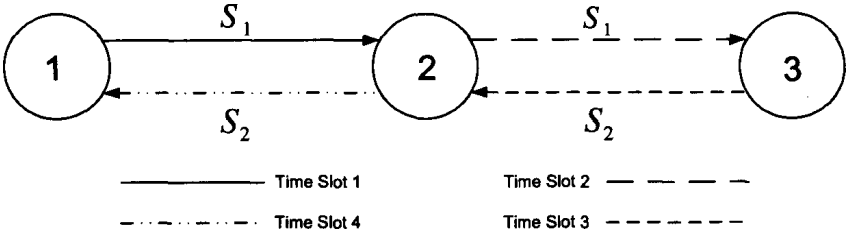

Figure 2.11: Traditional Scheduling Scheme

Let us assume that node-1 transmits information, S_1 to relay node in first time slot. During the second time slot, the relay node (node-2) relays that signal (S_1) to node-3. Node-3 then transmits its information, S_3 in third time slot to the relay node. In fourth time slot, relay node retransmits the information S_3 to node-1. In total it requires total four time slots to completely transmit information between two nodes.

Network Coding has then improved the scenario. Basically it was developed for the wireline communication system. and then it was used in wireless network to reduce the number of time slot for co-operative communication system. The idea is shown in figure-2.12.

At first time slot, node-1 transmits S_1 to relay node and then in the next time slot node-3 also sends S_3 to relay node. Once the relay receives S_1 and S_3, the relay

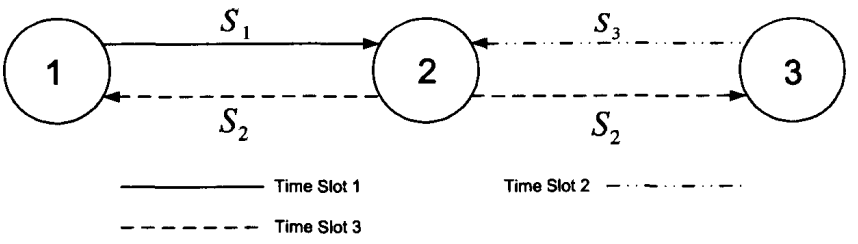

Figure 2.12: Network Coding Scheme

node encodes the signals as

$$S_2 = S_1 \oplus S_3 \tag{2.15}$$

where $\oplus$ denotes the bitwise XOR operation. Relay node then transmits the XORed signal to both source direction in the third time slot. When node-1 receives S_2, it extracts S_3 from S_2 using its own information S_1 as follows

$$S_1 \oplus S_2 = S_1 \oplus (S_1 \oplus S_3) = S_3 \tag{2.16}$$

In a similar manner node-3 will also extract the information sent from node-1. The only price it is required to pay is to store the information in the relay node.

Physical Network Coding can even reduce the required time slot into two. The scheme is represented in the figure-2.13.

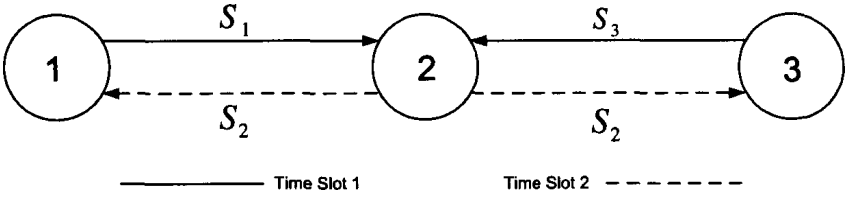

Figure 2.13: Physical Network Coding Scheme

As shown in the figure, at first time slot, both sources send information to the relay node simultaneously. The relay node receives the signals and then does XOR

operation. In the very next time slot, the relay node will transmit the XORed signal to both directions. After receiving the XORed signal, the source node retrieves the signal sent from the peer node by executing XOR operation with its own signal and the received signal from the relay node.

Our objective is now to elaborate the idea about Physical Network Coding. Let us assume that two sources S_1 and S_2 are to exchange information between them while R is the relay node as shown in figure-2.14. It is considered that the channel

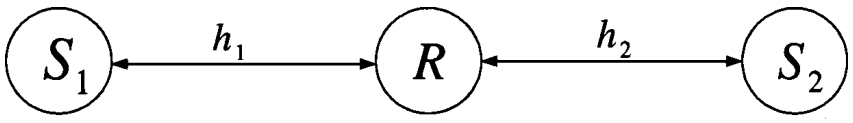

Figure 2.14: Co-operative Relay Network

gain does not change in two consecutive time slots. During first time slot, the received signal at relay node is given by

$$y_r = \sqrt{E_1}h_1S_1 + \sqrt{E_2}h_2S_2 + n \tag{2.17}$$

where,

E_1 = Transmission energy of node-1

E_2 = Transmission energy of node-2

h_1 = channel gain between node-1 and relay

h_2 = channel gain between node-2 and relay

S_1 = bpsk $0, 1 \in 1, -1$ modulated information of node-1

S_2 = bpsk $0, 1 \in 1, -1$ modulated information of node-2

n = Additive White Gaussian Noise

For simplicity it is assumed that $|h_1| > |h_2|$ [19] such that the signal constellation becomes similar as the figure-2.15.

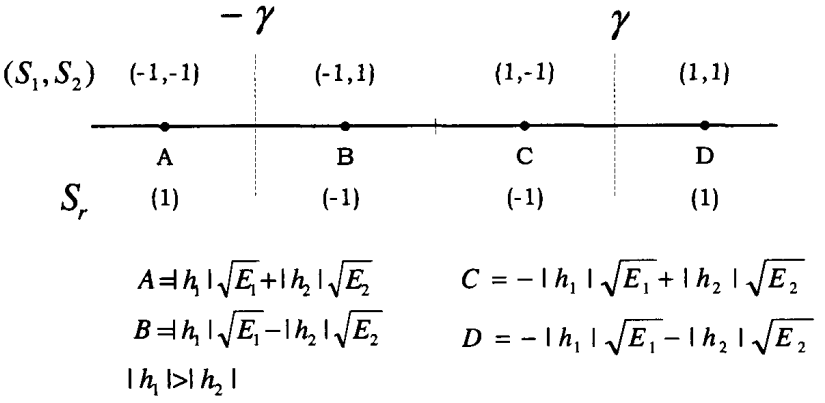

Figure 2.15: Signal Mapping at Relay Node

As shown in the figure, γ indicates the decision boundary to map S_r which is the XORed version of the signals sent from the sources. When the received signal y_r falls within the boundary $[-\gamma, \gamma]$, then S_r will be -1 and when y_r falls outside of that boundary, then S_r will be 1. In other words, when $[S_1, S_2]$ will equal to $[1, -1]$ or $[-1, 1]$, S_r will be -1 and when $[S_1, S_2]$ will equal to $[1, 1]$ or $[-1, -1]$, S_r will be 1. Once this decision is made, S_r is sent in both directions. So received signal at the source nodes will be

$$y_i = \sqrt{E_r} h_i S_r + n_i \tag{2.18}$$

where $i = 1, 2$ and E_r is the relay transmission energy.

When the source node i will receive y_i, it will detect the signal sent from the relay node. Then it would do XOR operation with its own signal and detect the signal sent from the peer node.

Performance is evaluated by simulation according to the process described previously. Figure-2.16 shows the performance curves for co-operative communication

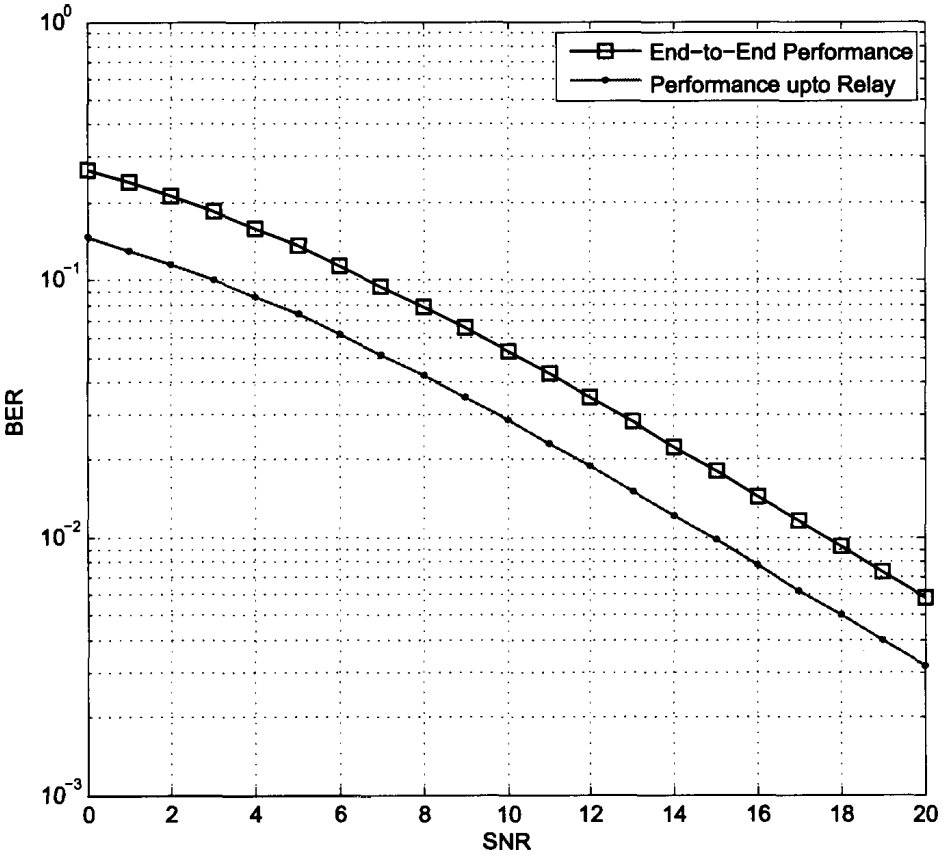

Figure 2.16: Performance of Physical Network Coding

system. Two curves are shown in the figure. One represents the end to end performance while the other one represents performance curve for source to relay node transmission performance.

2.4 Conclusion

In this chapter, basic ideas on the major topics related to the main research topic were discussed. Based on the topics covered in this chapter, the next chapters will explain more on those topics.

Chapter 3

Performance of MIMO system with Noisy Channel Estimation

The technology utilizing multiple antennas and space time block code has been developed to improvise the spectral efficiency of the wireless communication system [20]. Using multiple antennas wireless communication system eventually increases the reliability and the data rate of the system [21]. That is why it has created a lot of attention among the research community as well as industrial community over the last decade [14]. A simple diversity scheme proposed by Almaouti [2] had raised significant interest due to its simplicity and low complexity in design. In [2], the system is designed in such a manner that, under perfect CSI and quasi-static fading condition, it can eradicate interference completely and yield same performance as more complex Maximum Likelihood-Space Time Decoder (ML-STD) [2, 22]. However this scenario may not always be compared with the real system. While the channel is not quasi-static, the interference is not totally removed by this system even the CSI is perfect causing degradation in performance [23].

Another important factor which can degrade the performance of this scheme is imperfect estimation of the channel that basically occurs due to imperfect reception of pilot symbols. Under such condition, ML symbol detector with an interference suppression scheme or ML space time decoder can be used to mitigate this effect [17]. The situation can be even worse once the channel changes very rapidly. When channel

fades very rapidly at high Doppler frequency, channel estimation from the pilot symbol is no more reliable which degrades the system performance. It is desirable to evaluate the performance of Space Time Transmit Diversity (STTD) system considering the relationship between the Doppler frequency and channel estimation error and their impacts on the interference in the system.

In this chapter, a generalized model of the existing system has been shown and analytical performance of conventional Alamouti Space Time Code has been provided while considering imperfect CSI as well as time varying channels.

3.1 Some Definitions

Throughout the chapter, the following notation will be used. The upper-case bold letter denotes a matrix while a lower-case bold letter denotes a column vector. The element of m^{th} row and n^{th} column of a matrix $\mathbf{X}$ is represented by $\mathbf{X}(m,n)$. The superscripts T,H and * imply the matrix transpose, the matrix hermitian and the complex conjugate respectively. The determinant of a matrix $\mathbf{X}$ is defined as $|\mathbf{X}|$ while the square zero matrix and the square identity matrix of size n is denoted by $\mathbf{0}_n$, $\mathbf{I}_n$ respectively.

3.1.1 Characteristic Function of a Gaussian Variable

Let x is a zero-mean complex Gaussian random vector of length m and Q is a square matrix of order m and $\mathbf{\Sigma}$ be the covariance matrix of x, then the characteristic function of $z = x^H Q x$ can be given by [24]

$$\Phi_z(s) = |\mathbf{I}_m - 2s\mathbf{\Sigma Q}|^{-1} \tag{3.1}$$

3.1.2 Residue Theorem

Probability of z being less than zero can be found by Mellin's inversion formula and the residue theorem

$$Pr[r < 0] = \int_{\epsilon-\infty}^{\epsilon+\infty} \frac{j\Phi_z(s)}{2\pi s}\, ds = -\sum_{i=1}^{n_q} \text{Res}\left[\frac{\Phi_z(s)}{s} \text{ at } q_i\right] \tag{3.2}$$

Here n_q denotes the number of negative poles of $\Phi_z(s)/s$; q_i denotes i^{th} negative pole of $\Phi_z(s)/s$. Residue can be calculated by [25]

$$\text{Res}\left[f(s) \text{ at } a\right] = \lim_{s\to a} \frac{p^{(m-1)}(s)}{(m-1)!} \tag{3.3}$$

where $p(s) = (s-a)^m f(s)$ and $p^m(s)$ represents m^{th} derivative of $p(s)$.

3.1.3 Gauss-Chebyshev approximation

When the poles are closer or there are poles with higher order, it may not be practical to determine error probability by residue theorem. In such case, the probability that z is less than zero can be calculated from the Gauss-Chebyshev approximation [26],

$$P_r(z < 0) \approx \frac{1}{2m} \sum_{k=1}^{m} (\Re[\Phi_z(\epsilon + j\epsilon\tau_k)] + \tau_m \Im[\Phi_z(\epsilon + j\epsilon\tau_k)]) \tag{3.4}$$

where $\Re[x]$ and $\Im[x]$ represent the real and the imaginary parts of x respectively. $\tau_k = tan((2k-1)\pi/4m)$, ϵ lines between the left half-plane poles and the imaginary axis and normally the value of m between 16 and 32 is sufficient [26].

3.2 System Model

For the analysis of our study, it has been considered that the system is BPSK DS-CDMA system with two antenna at the transmission end while one antenna at the reception side. Elaborated discussion on Transmitter, Channel, Receiver is given in this section.

3.2.1 Transmitter

As specified earlier there are two transmit antennas at base station and those are placed with sufficient space so that the information sent from the transmitters are uncorrelated. Information bits are encoded by the Alamouti's Space Time Encoder [2] and then transmitted. Complex conjugate of the signals used in Alamouti's STBC can be ignored as BPSK system is of the interest. Both transmit antennas use the same orthogonal code for transmitting data sequence. Unlike the data sequence, while transmitting pilot sequence, each transmit antenna sends distinct codes since each antenna has to estimate the channel condition separately. For simplicity of the

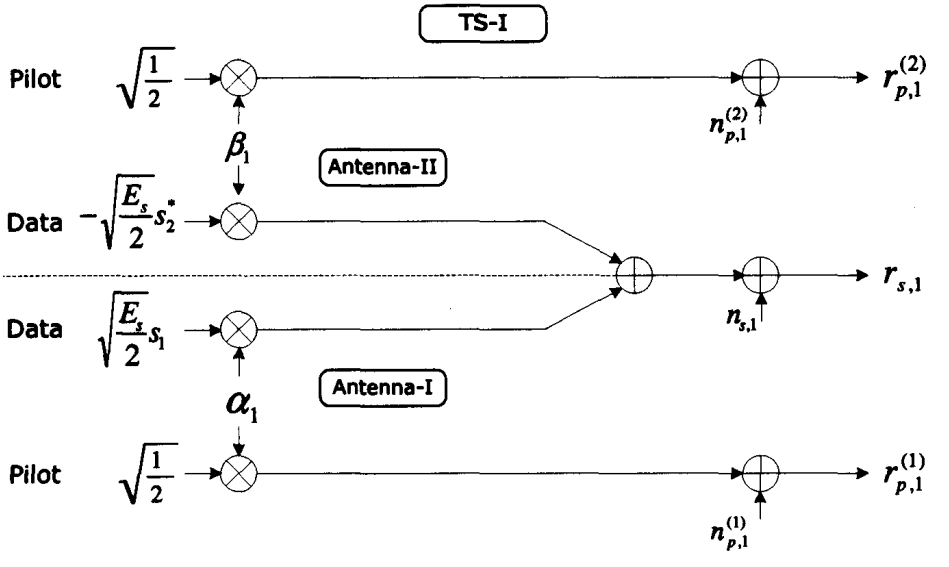

Figure 3.1: System Model for MIMO system with pilot symbol during first time slot

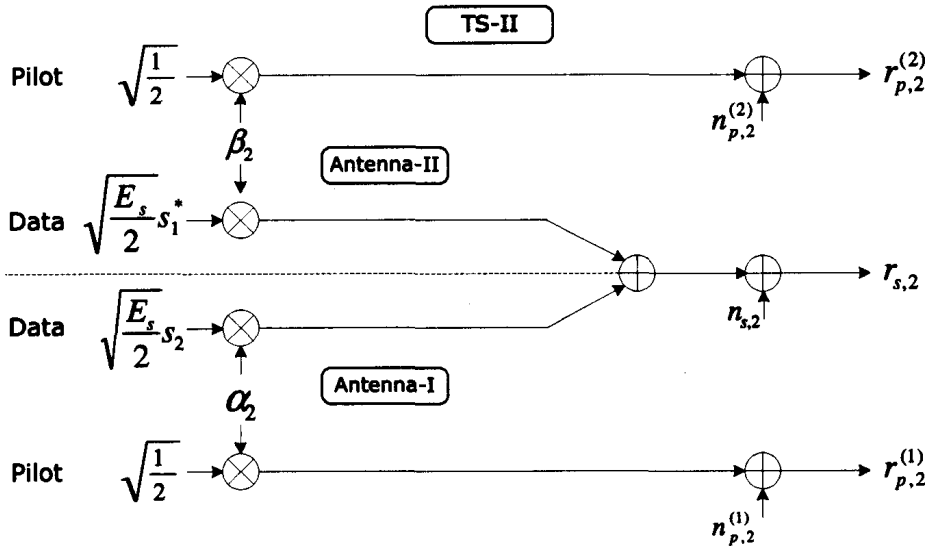

Figure 3.2: System Model for MIMO system with pilot symbol during second time slot

analysis, it is assumed that both data channels and pilot channels have the same spreading gain which implies that both will have same time period τ. The system is represented in figure-3.1 and 3.2.

The transmitted sequence of modified Alamouti's space time code [17] is given in Table-3.1

Table 3.1: Modified Alamouti Space Time Code

Symbol Time	Antenna 1	Antenna 2
1	s_1	$-s_2^*$
2	s_2	s_1^*

Here s_k denotes the data bit during the time index of k. E_s represents energy per transmitted data symbols. Equivalently energy per symbol for each antenna will be $E_s/2$ for data symbol and $1/2$ for pilot symbol.

3.2.2 Channel

It is assumed that the channels are time-varying Rayleigh fading channels. Fading co-efficients are assumed to be zero-mean circularly symmetric complex Gaussian random variables. The fading co-efficient of the channel between the first transmit antenna and the receiver is denoted by α_k and between the second transmit antenna and the receiver is represented by β_k where the subscript k represents time index. It is assumed that α_k and β_k are uncorrelated with identical autocorrelation $\sigma_c^2 R(m)$ where $R(0)$ is normalized to unity. Although time varying channels are assumed, in this study, it is considered that channel fades in such a manner that channel does not change during the symbol period.

3.2.3 Receiver

Received signal experiences the effect of noise at the reception side. Noise in the data channel and the pilot channel from transmit antenna A and transmit antenna B are represented by $n_{s,k}$, $n_{p,k}^1$ and $n_{p,k}^2$. All are complex white Gaussian variables with variances σ_s^2, σ_p^2 and σ_p^2 respectively. The baseband representation of the received signals assuming that the channels are flat-fading can be expressed as

$$\mathbf{r_s} = \begin{bmatrix} r_{s,1} \\ r_{s,2}^* \end{bmatrix} = \sqrt{\frac{\mathbf{E_s}}{\mathbf{2}}} \begin{bmatrix} \alpha_1 & -\beta_1 \\ \beta_2^* & \alpha_2^* \end{bmatrix} \begin{bmatrix} s_1 \\ s_2^* \end{bmatrix} + \begin{bmatrix} n_{s,1} \\ n_{s,2}^* \end{bmatrix}$$

$$r_{p,i}^1 = \frac{1}{\sqrt{2}}\alpha_i + n_{p,i}^1 \rightarrow \mathbf{r_{p,i}^1} = \left[r_{p,i-M}^1 \cdots r_{p,i}^1 \cdots r_{p,i+M}^1 \right] \tag{3.5}$$

$$r_{p,i}^2 = \frac{1}{\sqrt{2}}\alpha_i + n_{p,i}^2 \rightarrow \mathbf{r_{p,i}^2} = \left[r_{p,i-M}^2 \cdots r_{p,i}^2 \cdots r_{p,i+M}^2 \right]$$

Here the subscript i, p and s indicate the time index, the pilot channel and the data channel respectively while the superscripts 1 and 2 indicate the quantity belonging to the first antenna and second antenna.

At the reception side, the channel can be estimated by $(2M+1)$-tap FIR filters. The output of the FIR filter can be expressed as

$$\hat{\alpha}_i = \mathbf{h}^H \mathbf{r}^1_{p,i}, \quad \hat{\beta}_i = \mathbf{h}^H \mathbf{r}^2_{p,i} \tag{3.6}$$

where $\hat{\alpha}_i$ and $\hat{\beta}_i$ represents the estimated channel from first and second antenna respectively and $\mathbf{h} = [h_M \ \cdots \ h_0 \ \cdots \ h_{-M}]^T$ indicates the pilot filter co-efficients.

3.3 Linear Combining Scheme

Linear Combining Space-Time Decoder (LC-STD) suggested by Alamouti [2] is the simplest among all due to its low complexity [13]. This section will demonstrate the derivation of the error probability of Alamouti's scheme where LC-STD is considered.

The linear combining scheme which is suggested by Alamouti [2] can be expressed in the vector form as

$$\begin{bmatrix} z_1 \\ z_2^* \end{bmatrix} = \begin{bmatrix} \hat{\alpha}_1^* & \hat{\beta}_2 \\ -\hat{\beta}_1^* & \hat{\alpha}_2 \end{bmatrix} \mathbf{r_{s,1}} = \sqrt{\frac{\mathbf{E_s}}{\mathbf{2}}}\, \mathbf{G} \begin{bmatrix} s_1 \\ s_2^* \end{bmatrix} + \begin{bmatrix} \tilde{n}_{s,1} \\ \tilde{n}_{s,2} \end{bmatrix} \tag{3.7}$$

Here z_1 and z_2 are the output of the linear combiner corresponding to the first and second data symbols. In addition, $\tilde{n}_{s,1} = \hat{\alpha}_1^* n_{s,1} + \hat{\beta}_2 n_{s,2}$, $\tilde{n}_{s,2} = \hat{\beta}_1^* n_{s,1} + \hat{\alpha}_2 n_{s,2}^*$

and

$$\mathbf{G} = \begin{bmatrix} \alpha_1\hat{\alpha}_1^* + \beta_2^*\hat{\beta}_2 & \alpha_2^*\hat{\beta}_2 - \beta_1\hat{\alpha}_1^* \\ \beta_2^*\hat{\alpha}_2 - \alpha_1\hat{\beta}_1^* & \beta_1\hat{\beta}_1^* + \alpha_2\hat{\alpha}_2^* \end{bmatrix} \tag{3.8}$$

In the case of perfect CSI and quasi static channels with $\alpha_1 = \alpha_2$ and $\beta_1 = \beta_2$, the linear combining scheme can eradicate the interference completely [17]. Hence $\mathbf{G}$ becomes to

$$\mathbf{G_{perfect}} = \begin{bmatrix} |\alpha_1|^2 + |\beta_1|^2 & 0 \\ 0 & |\alpha_1|^2 + |\beta_1|^2 \end{bmatrix} \tag{3.9}$$

Without loss of generality, it can be assumed that $s_1 = s_2 = 1$. Since the bit error probability of the first symbol and the bit error probability of the second symbol are the same, only one symbol can be taken into account to derive the error probability. Let us assume the case for first symbol. From (3.7), the output of the linear combiner corresponding to the first symbol is

$$z_1 = \hat{\alpha}_1^* r_{s,1} + \hat{\beta}_2 r_{s,2}^* \tag{3.10}$$

In quadratic form, the real part of z_1 can be written as $Re[z_1] = \mathbf{x}^H\mathbf{Q}\mathbf{x}$ [17] where

$$\mathbf{x} = \begin{bmatrix} r_{s,1} & r_{s,2} & \hat{\alpha}_1 & \hat{\beta}_2 \end{bmatrix}^T \tag{3.11}$$

and

$$\mathbf{Q} = \frac{1}{2}\begin{bmatrix} \mathbf{0_2} & \mathbf{I_2} \\ \mathbf{I_2} & \mathbf{0_2} \end{bmatrix} \tag{3.12}$$

Using the ML symbol detector, error would occur when $Re[z_1]$ or $\mathbf{x^H Q x}$ is less than zero. The bit error probability P_b can be expressed as

$$P_b = Pr\left[\mathbf{x}^H \mathbf{Q x} < 0\right] \tag{3.13}$$

The characteristic function of $\Re[z_1]$ can be determined from Section-3.1.1. Here it is required to know the covariance matrix of $\mathbf{x}$. After some calculation, the covariance matrix $\mathbf{\Sigma}$ was found as

$$\mathbf{\Sigma} = \begin{bmatrix} \mathbf{A} & \mathbf{C} \\ \mathbf{C}^H & \mathbf{B} \end{bmatrix} \tag{3.14}$$

where

$$\mathbf{A} = E_s \sigma_c^2 (1 + \bar{\gamma}_s^{-1}) \mathbf{I_2}$$

$$\mathbf{B} = \sigma_c^2 \, \mathbf{h}^H \left(\frac{\mathbf{D_0}}{2} + \bar{\gamma}_p^{-1} \mathbf{I}_{2M+1}\right) \mathbf{h} \, \mathbf{I_2} \tag{3.15}$$

$$\mathbf{C} = \frac{\sqrt{E_s}\sigma_c^2}{2} \begin{bmatrix} \mathbf{w}_0^H \mathbf{h} & -\mathbf{w}_1^H \mathbf{h} \\ \mathbf{w}_{-1}^H \mathbf{h} & \mathbf{w}_0^H \mathbf{h} \end{bmatrix}$$

Here $\bar{\gamma}_p = \sigma_c^2/\sigma_p^2$ represents the average pilot Signal to Noise Ratio (SNR) or pilot E_p/N_0 and $\bar{\gamma}_s = E_s\sigma_c^2/\sigma_s^2$ denotes the average data SNR or data E_b/N_0. $\mathbf{D_e}$ is a square matrix of order $2M+1$ with $\mathbf{D}_e(i,j) = R((e+i-j)\tau)$ and $\mathbf{w}_e$ is the $(M+1)^{th}$ column of $\mathbf{D}_e$. After knowing $\mathbf{\Sigma}$, P_b can be calculated by using residue theorem described in Section-3.1.2 or by Gauss-Chebyshev approximation described in Section-3.1.3.

For the simplicity of the analysis for calculating bit error probability, $(2M+1)$-tap Wiener filter as a pilot filter is considered throughout the study. While using the Wiener filter, the filter co-efficient becomes

$$\mathbf{h} = \frac{1}{\sqrt{2}}(\frac{\mathbf{D}_0}{2} + \bar{\gamma}_p^{-1}\mathbf{I}_{2M+1})^{-1} \tag{3.16}$$

Putting the value of $\mathbf{h}$ in (3.15) and then replacing the values of A, B and C in(3.14) will yield

$$\mathbf{\Sigma} = \sigma_c^2 \begin{bmatrix} E_s(1+\bar{\gamma}_s^{-1})\,\mathbf{I}_2 & \sqrt{\frac{E_s}{8}} \begin{bmatrix} \varepsilon_0 & -\varepsilon_1 \\ \varepsilon_1 & \varepsilon_0 \end{bmatrix} \\ \begin{bmatrix} \varepsilon_0 & \varepsilon_1 \\ -\varepsilon_1 & \varepsilon_0 \end{bmatrix} & \frac{\varepsilon_0}{2}\mathbf{I}_2 \end{bmatrix} \tag{3.17}$$

where

$$\varepsilon_0 = \mathbf{w}_0^H\,(\frac{\mathbf{D}_0}{2} + \bar{\gamma}_p^{-1}\mathbf{I}_{2M+1})^{-1}\,\mathbf{w}_0 \tag{3.18}$$

$$\varepsilon_1 = \mathbf{w}_1^H\,(\frac{\mathbf{D}_0}{2} + \bar{\gamma}_p^{-1}\mathbf{I}_{2M+1})^{-1}\,\mathbf{w}_0 \tag{3.19}$$

After some calculations, the eigenvalues of $2\mathbf{\Sigma Q}$ can be found as

$$\lambda_1 = \sigma_c^2\varepsilon_0(1+\Upsilon^{-1}) \tag{3.20}$$

$$\lambda_2 = \sigma_c^2\varepsilon_0(1-\Upsilon^{-1}) \tag{3.21}$$

both are of order two and

$$\Upsilon = \left(\frac{4(1+\bar{\gamma}_s^{-1})}{\varepsilon_0} - \left(\frac{\varepsilon_1}{\varepsilon_0}\right)^2\right)^{-\frac{1}{2}} \tag{3.22}$$

The eigen values are necessary to calculate the poles of the characteristic function. From the equation (3.20), (3.21) and (3.22), it can be shown that the poles of the characteristic function are at 0, $1/\lambda_1$ and $1/\lambda_2$. From the inspection it can be stated that $1/\lambda_2$ is in LHP and $1/\lambda_1$ is in RHP. Hence from the residue theorem P_b is equal to residue of $\Phi(s)/s$ with negative sign at $1/\lambda_2$.

It can be shown that the residue is invariant to the scaling of the poles (see the appendix for the proof). Using this the compact form of the bit error probability with scaling factor $\sigma_c^2\varepsilon_0$ can be calculated as

$$P_b = \lim_{x \to \frac{\sigma_c^2\varepsilon_0}{\lambda_2}} \frac{d}{ds}\left(\frac{(s-\frac{\sigma_c^2\varepsilon_0}{\lambda_2})^2}{s(1-\frac{s\lambda_1}{\sigma_c^2\varepsilon_0})^2(1-\frac{s\lambda_2}{\sigma_c^2\varepsilon_0})^2}\right) \tag{3.23}$$

After some calculation the expression for the bit error probability becomes

$$P_b = \frac{1}{4}(2+\Upsilon)(1-\Upsilon)^2 \tag{3.24}$$

This result can be compared with perfect CSI result by setting $\bar{\gamma}_p \to \infty$. This would result the value for ε_0, ε_1 as 2, $2R(\tau)$ respectively and

$$\Upsilon = (2 + 2/\bar{\gamma}_s - R^2(\tau))^{-1/2} \tag{3.25}$$

Two types of channel can be considered to get the bit error probability. One is when $R(\tau) = 0$ which implies very fast fading or $R(\tau) = 1$ which basically means that static channel is under consideration with perfect knowledge of the channel in both cases. Therefore, from equation (3.25) and (3.24), it can be written

$$R(\tau) = 0 \to P_b = \frac{1}{4}\left(2 + \sqrt{\frac{\bar{\gamma}_s}{2\bar{\gamma}_s+2}}\right)\left(1 - \sqrt{\frac{\bar{\gamma}_s}{2\bar{\gamma}_s+2}}\right)^2 \tag{3.26}$$

$$R(\tau) = 1 \rightarrow P_b = \frac{1}{4}\left(2 + \sqrt{\frac{\bar{\gamma}_s}{\bar{\gamma}_s + 2}}\right)\left(1 - \sqrt{\frac{\bar{\gamma}_s}{\bar{\gamma}_s + 2}}\right)^2 \tag{3.27}$$

The result obtained from equation (3.27) matches with the result derived in [22] and [27]

Bit error probability of s_1 and s_2 are equal, however, they are not independent. The upper bound of the block error probability of Alamouti code is

$$P_{alamouti} \leq 2P_b \tag{3.28}$$

It is assumed that fading correlation function is the zeroth-order Bessel function of the first kind $J_0(2\pi f_D \tau)$ which is basically derived from Jakes' PSD [1]. It is for simplistic analysis when it is considered that the wireless environment is have isotropic scattering which basically implies that signals are coming to the receiver from all direction. However in real scenario the signals may come to the receiver from a fixed direction which is named as directional scattering. While considering directional scattering some other parameters are considered for the correlation function. The correlation function becomes [28]

$$R(\tau) = I_0\left(\sqrt{\kappa^2 - 4\pi^2 f_D^2 \tau^2 + j4\pi\kappa\cos(\mu) f_D \tau}\right)/I_0(\kappa) \tag{3.29}$$

where $I(.)$ is the zeroth-order modified Bessel function. μ represents the mean direction of Angle of Arrival (AOA) and $\kappa \geq 0$ controls the width of AOA [29]. When it is considered that isotropic scattering, the value of κ is equal to 0 while for extreme non-isotropic scattering the value of κ is ∞.

3.4 Simulation and Results

Simulations have been done according to the expression obtained from the previous sections to illustrate the effect of the Doppler spread and the channel estimation error on the performance of the Space Time Code. At first it is considered for isotropic scattering which is shown in figure-3.3 which represents the performance curves for the linear combining scheme.

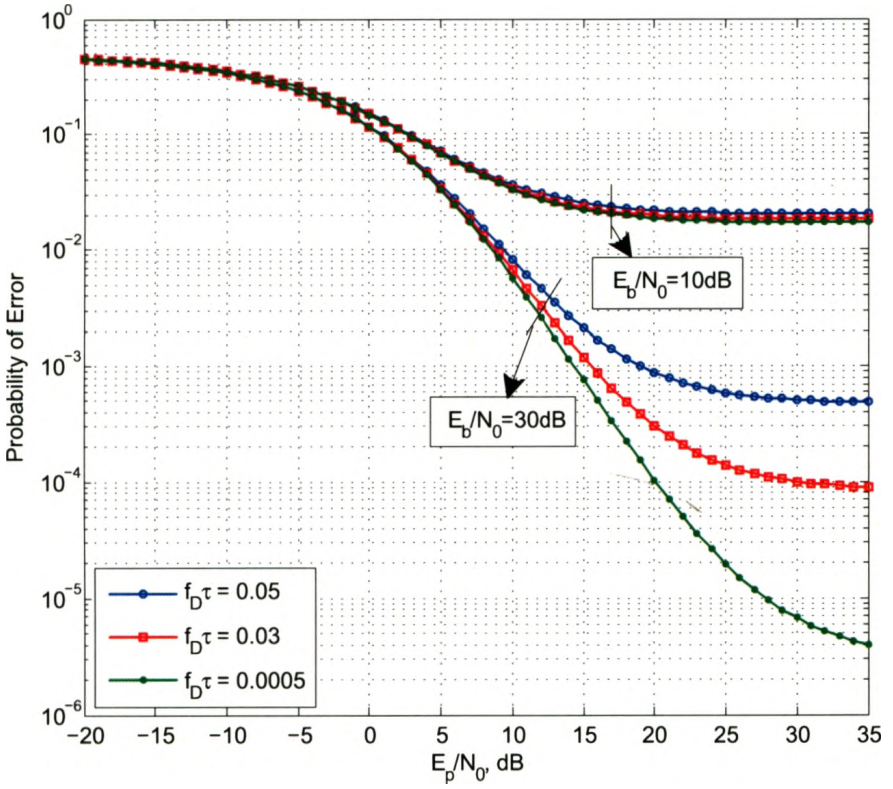

Figure 3.3: Effect of Doppler Spread on Alamouti's Space Time Code in Isotropic Environment

Pilot SNR is varied and the error probability is measured to determine the performance of the system. The simulation results are represented with the bounds for $f_D\tau = 0.0005$, 0.03 and 0.05 which are presented by green, red and blue lines, respectively. Certainly when the data SNR is more, the performance is better. That is why the performance curves under data SNR $= 30dB$ is better than that of data

SNR $= 10dB$. When the channel is about to be quasi-static (value of $f_D\tau$ is less), the system performs better. As the channel becomes more dynamic, the system performance degrades. At high pilot SNR, the error probability value becomes almost constant since beyond a certain point pilot SNR does not play any role to improve the performance.

Till now the performance has been shown for isotropic scattering environment. Performance curves for non-isotropic environment are shown in figure-3.4, 3.5 and 3.6. In those curves it is tried to investigate how the performance varies when doppler spread or angle of arrival or width of angle of arrival is changed. For all cases, pilot SNR is fixed at $30dB$ and data SNR is varied to analyse the performance of the system.

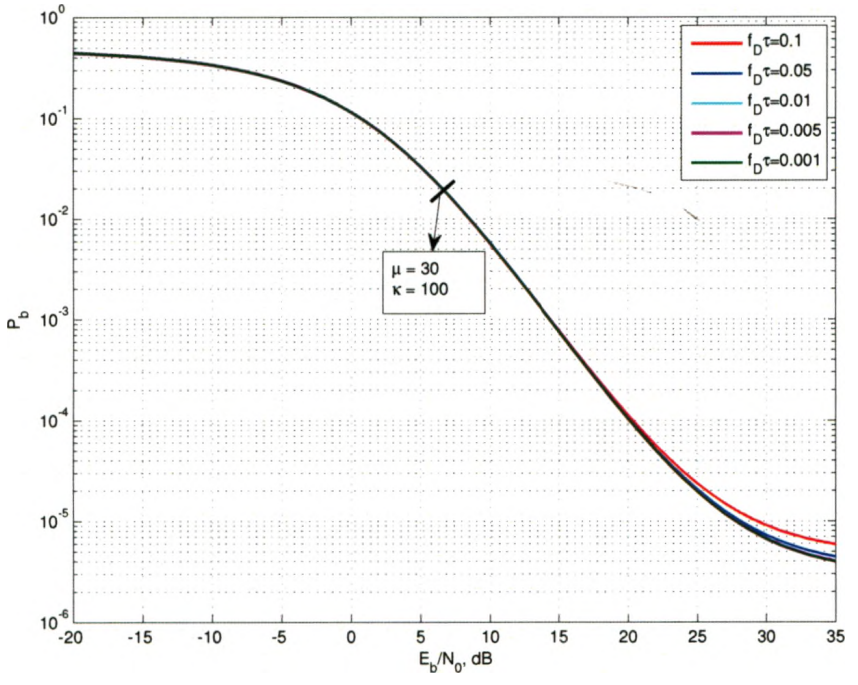

Figure 3.4: Effect of Doppler Spread on Alamouti's Space Time Code in Non-isotropic Environment

Figure-3.4 shows the performance graphs while varying the Doppler spread. In this case the value of κ is fixed at 100 and the value of μ is taken 30. Different

values of Doppler spread gave different result. As the Doppler Spread is increasing the system performance is getting worse. When the Doppler Spread is increasing, it means that the signal is experiencing more fading. And when it experiences more fading, certainly the performance will deteriorate.

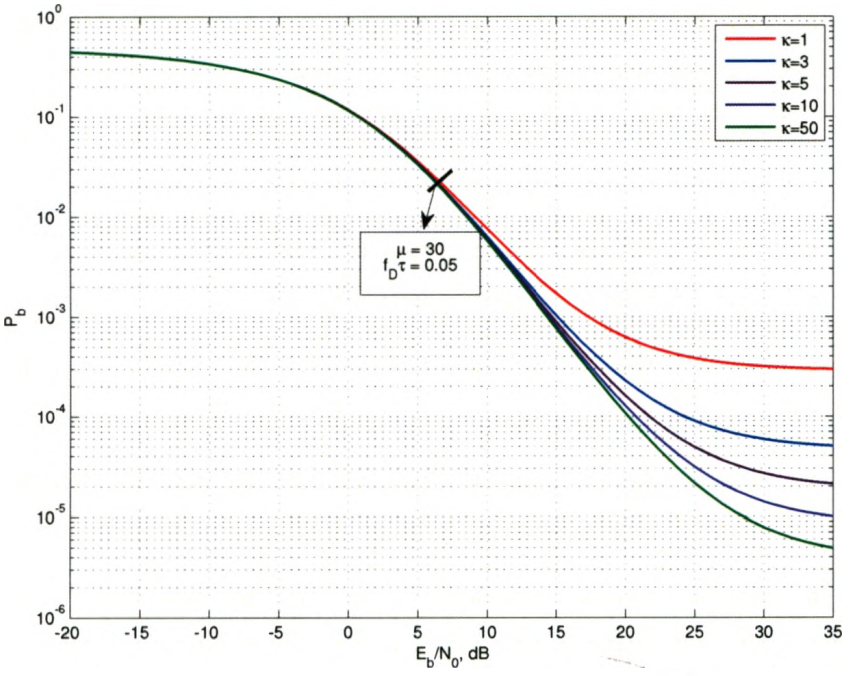

Figure 3.5: Effect of κ on Alamouti's Space Time Code in Non-isotropic Environment

Figure-3.5 represents the system performance when the width of angle of arrival is varied. To investigate such scenario the value of $f_D\tau$ is taken to be 0.05 and the value of μ is considered 30. It is seen from the figure that as the value of κ is increasing the overall system performance is improving. Since the width of angle of arrival is increasing, the performance is getting better.

Performance of a system while varying the angle of arrival is demonstrated in figure-3.6. For this case κ is fixed at 30 while the value of $f_D\tau$ is taken 0.05. Results show that as the angle of arrival is reducing, the performance of the system is improving. When the angle of arrival is large, the receiver will receive transmitted signal

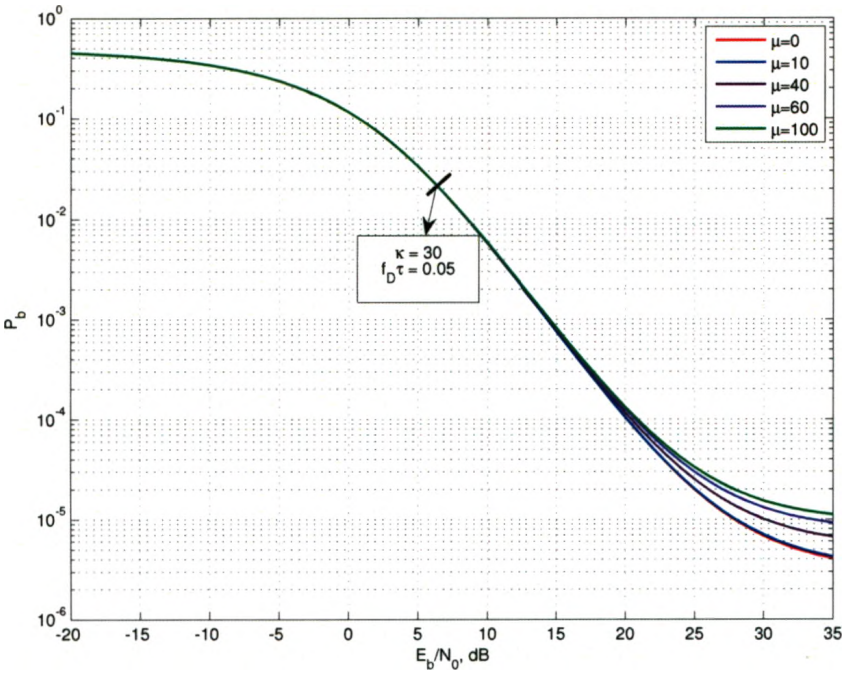

Figure 3.6: Effect of μ on Alamouti's Space Time Code in Non-isotropic Environment

from a bigger angle and hence receive required information signal as well as more unwanted signals simultaneously. Due to this factor, system performance degrades with the increment of angle of arrival.

3.5 Conclusion

In this chapter, it was investigated how the wireless system performs with Alamouti's scheme by deriving the bit error probability theoretically. The channel was considered as time varying Rayleigh faded channel. In Alamouti's scheme, it was considered that channel state does not change in consecutive two time slots which may not be practical in all scenarios. To analyze the overall system performance comparable to the real situation, it was assumed that the channels are not quasi-static since the channel condition can change at any instant of time. Another thing which is also different

from traditional analysis is about the pilot signals. It is considered that pilot signals might be erroneous which is sometimes ignored in some studies. The effect of channel estimation error and the channel condition on the system performance are evaluated. System performance is basically analyzed for isotropic scattering environment. Later system performance was evaluated for more realistic case, non-isotropic scattering, where some other parameters like Doppler frequency, angle of arrival, width of angle of arrival etc. are considered. It has been observed that those parameters play good role in the overall system performance.

Chapter 4

Effect of Impulse Noise in Co-operative Diversity System

In wireless communication systems, signal fading arising from multipath propagation is one of the major performance-limiting factors. Fading severely degrades the link performance and hence to maintain an acceptable level of performance, powerful countermeasures such as diversity techniques should be employed. Spatial diversity which basically involves with multiple transmit or receive antennas is commonly used to improve the link reliability, throughput in wireless systems. In many applications where spacing does limit the deployment of multiple antennas at transmission or reception end, cooperative diversity can be considered an effective fading-mitigation technique. [30–33].

Co-operative diversity has shown its ability to improvise system performance in terms of transmission reliability, system capacity, coverage area extension etc. As such it has attracted considerable attraction in recent years [34]. The idea of co-operative communication was first proposed in Van der Meulen's work [35]. Since then numerous researches were done to utilize the maximum benefits from this technique. In co-operative relay network two sources exchange their information with help of at least one node, which is called relay [36]. There are several schemes used in co-operative relay network namely Amplify and Forward (AF) [37], Denoise and Forward (DF) [38] which is also known as Physical Network Coding (PNC) [39], Analog

Network Coding (ANC) [40] etc. Depending upon the requirements of the network system, different scheme can be used.

An important noticeable matter about co-operative diversity is that co-operative diversity is studied only in a such condition where Additive White Gaussian Noise (AWGN) is considered. However the real scenario might be different depending upon the environment condition. Practically AWGN represents the thermal noise at the receiver while it does not consider the impulsive nature of the environment which can even degrade the system performance drastically. In many industrial applications as well as some radio scenarios, the system is characterized by a noise which exhibits the impulsive nature of the environment. It is not possible to describe this by AWGN model. This phenomena is referred to as impulse noise and it can be described by either Class-A model [41] or Bernoulli-Gaussian model [15]. Our concern with impulse noise will mainly be encompassing Bernoulli-Gaussian model.

A new era is going to be started where diversity is blended with the co-operative system. It can reap the benefit from both diversity technique as well as co-operative relay system. It is well known that protocols with Multiple Access (MAC) and the broadcast (BC) phases in a bi-directional relay system can attain a higher spectral efficiency than the conventional protocols which use basically three or four phases [42]. A physical layer network coding (PNC) is used in [39], [43] to exchange information efficiently in a situation where the relay node detects and then forwards the XOR-like version of a pair of transmitted symbols. Ju *et al.* had derived upper and lower bounds on symbol error probability for the system with single antenna system in each node [36]. Authors described a model in [44] considering multiple antenna set at the relay end. In this thesis, multiple antennas will be under consideration at the transmission and reception end in a co-operative system.

4.1 Co-operative system in Impulsive Noise environment

In this section, co-operative system will be discussed in an impulsive noise environment. Physical-layer Network Coding (PNC) is to be considered for this analysis.

4.1.1 System Model

Let us consider a bidirectional relay network consisting of two sources and a relay. Each node has a single antenna and it operates in half duplex mode. S_1, S_2 and R are used to denote source-I, source-II and the relay respectively as shown in the figure-4.1

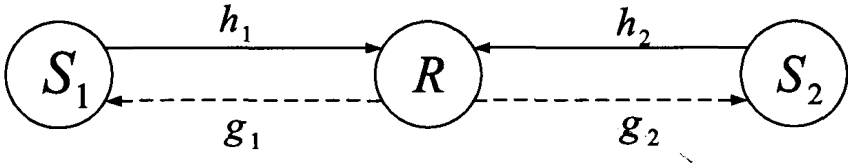

Figure 4.1: System Model for Co-operative Communication System

Let m_i denotes binary information from the source S_i. The BPSK modulated signal of S_i will then be $x_i = 1 - 2m_i$ where $m_i \in \{0,1\}$ and $x_i \in \{1,-1\}$ for $i = [1, 2]$. Let us denote the complex channel coefficient between S_i and R by h_i during first time slot and g_i during the second time slot. Channels can be modeled as $h_i \sim \mathcal{CN}(0, \sigma^2)$ for $i = 1, 2$ where $h \sim \mathcal{CN}(m, \omega)$ indicates h is circularly symmetric complex-valued Gaussian random variable with mean m and variance ω. For simplicity it can be assumed that channel coefficients are constant in two consecutive time slots. It means that $h_i = g_i$. It is assumed that the phase of the transmitted signals from S_1 and S_2 are synchronized at the relay node.

During first time slot, both S_1 and S_2 transmit their information x_1 and x_2 respectively to relay node R. The signal received by the relay node can be shown by

$$r = \sqrt{E_1}h_1x_1 + \sqrt{E_2}h_2x_2 + w + i \tag{4.1}$$

where E_i is the transmission power at S_i, w is the additive white Gaussian Noise (AWGN) and i is impulse noise which can be defined as Bernoulli-Gaussian Model [15]. It implies that impulse noise is the product of real Bernoulli process and a complex Gaussian process as following:

$$i = bg \tag{4.2}$$

where b is the Bernoulli process which is basically a random series of 0's and 1's with a probability of p occurring 1's. g is the complex White Gaussian Noise with mean zero. In this system, it is assumed $|h_1| > |h_2|$ [19] so that the received signal r at relay becomes the same as the figure-4.2.

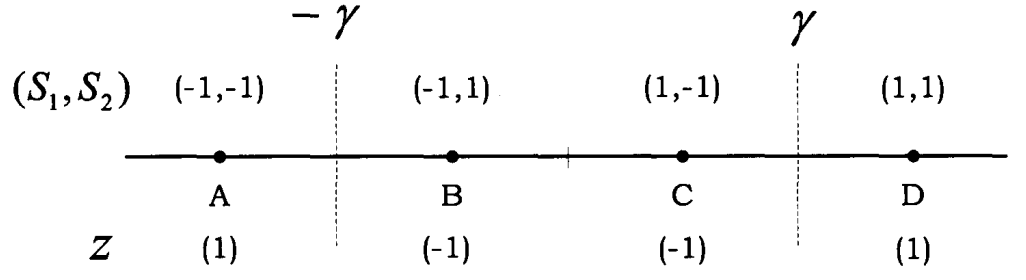

Figure 4.2: Constellation of Received Signal at Relay Node

From figure-4.2, γ defines the decision boundary to map z which is the information the relay transmits to both S_1 and S_2 during second time slot. When $[x_1, x_2]$ is equal to $[-1, 1]$ or $[1, -1]$, it will fall into the decision region [-γ, γ] and hence the

relay would transmit -1 towards both sources. Again when $[x_1, x_2]$ is equal to $[1, 1]$ or $[-1, -1]$, it will fall into the decision region outside of [-γ, γ] and the relay would transmit 1 towards both sources.

Once the mapping is done at the relay node, the relay forwards the XORed symbol z towards the sources over the BC. The signal received by S_i is given by

$$y_i = \sqrt{E_r} h_i z + n_i + w_i \tag{4.3}$$

where E_r means transmission power at relay, n_i means AWGN at S_i and w_i means IN at S_i. After receiving XORed signal from the relay node, source nodes S_1 and S_2 decode the received signal and detect the signal sent from peer node by executing XOR operation with the detected signal from relay node and its own signal.

4.1.2 Simulation and Result

In this section performance evaluation will be shown for co-operative relay communication system under Rayleigh fading condition with AWGN as well as IN environment. It will be shown in two steps. At first Signal to Noise Ratio (SNR) will be varied and corresponding Error Rate will be observed to analyze the system performance. In that case a fixed amount of Impulse Noise will be in effect for each value of SNR. Secondly Signal to Impulse noise Ratio (SIR) will be varied and similarly corresponding Error Rate will be observed to study the overall performance. In this case SNR will be fixed to a certain value.

4.1.2.1 Varying SNR

In this step error rate is measured while varying the value of SNR. The value of SIR is kept constant. Later the value of SIR is changed to another value to visualize how the performance changes. For a single value of SIR, different curves are considered by changing the value of p.

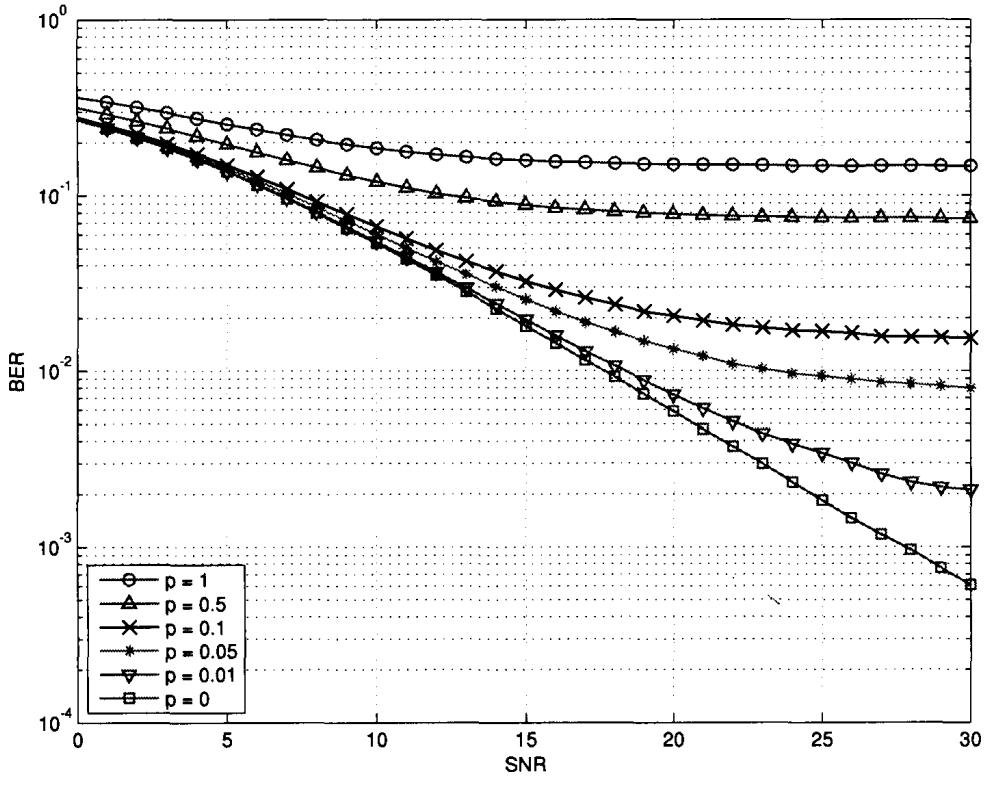

Figure 4.3: Effect of varying SNR in a co-operative communication system while SIR = 5dB

Figure-4.3, figure-4.4 and figure-4.5 represent the performance graphs of co-operative relay system in impulsive noise environment considering the value of SIR as 5dB, 10dB and 15dB respectively. For each case, when the value of p is increasing, the performance deteriorates. Basically p is the probability of adding impulse noise with the system. In other words p implies how frequently impulse noise is adding to the received signal. For example, when the value of p is equal to 1, it means that

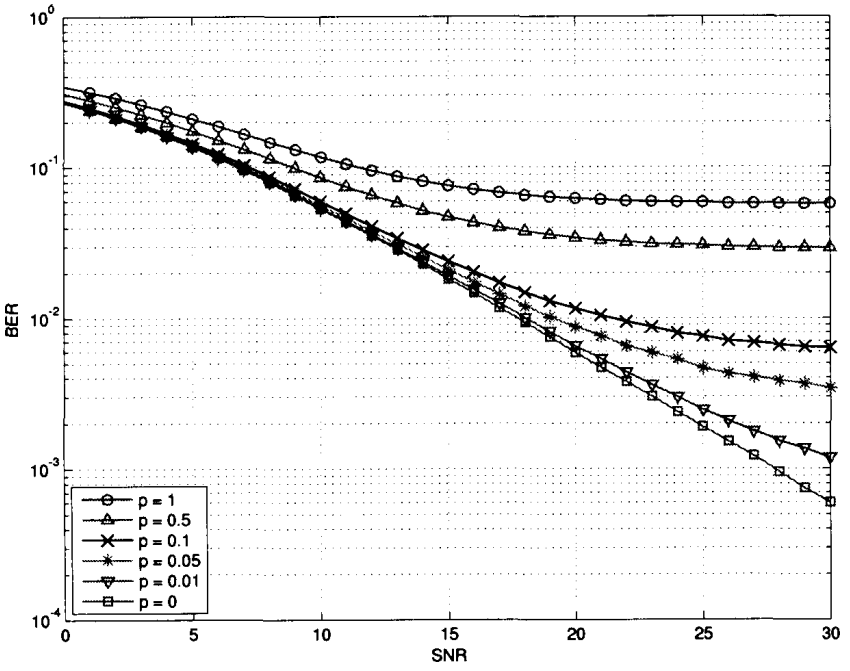

Figure 4.4: Effect of varying SNR in a co-operative communication system while SIR = 10dB

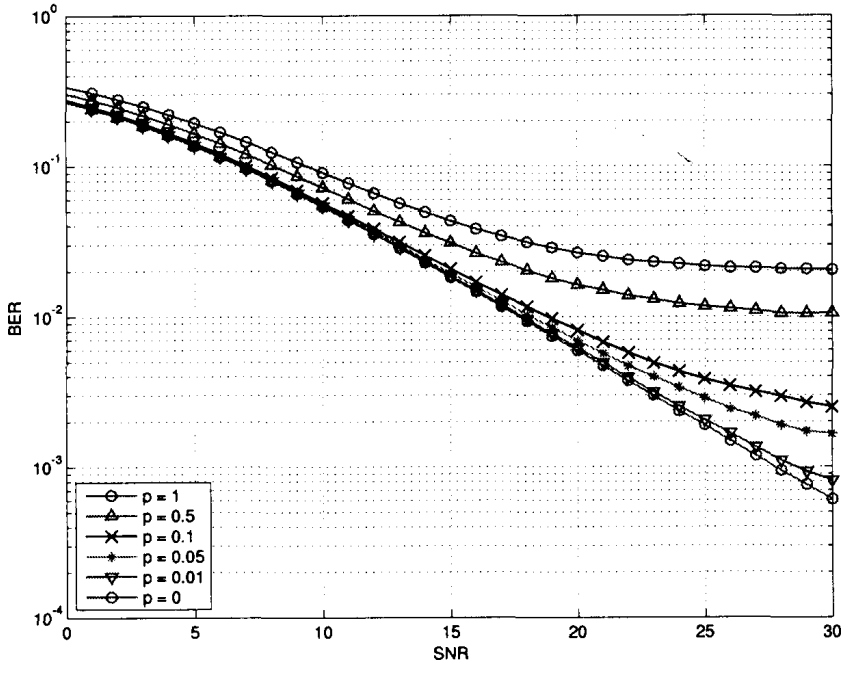

Figure 4.5: Effect of varying SNR in a co-operative communication system while SIR = 15dB

Impulse Noise is considered for each bit of the information stream. When p is equal to zero, it indicates that there is no impulse noise is added with the received signal.

As expected when the value of p is increasing from 0 to 1, the performance gradually deteriorates. Similarly when the value of SIR is increased, the performance improves since the signal strength is increasing or, in other words, impulse noise power is decreasing. It is also observed that while p has a value greater than 0 the graph saturates after a certain value. It is happening due to the fact that although the value of SNR is increasing which indicates less effect of noise, there is still a certain amount of impulse noise adding to the received signal. Since the increment of SNR does not have any hold on that, the performance curves saturate after a certain SNR value.

4.1.2.2 Varying SIR

Performance of the co-operative communication system is studied in this section while varying the value of SIR and putting the SNR into a fixed value. The value of SNR is then changed to another value to compare the system performance. For each scenario, the value of p is changed from 0 to 1 to analyze the impact of impulse noise to the system.

Three different scenarios are considered to investigate the overall system performance while varying SIR. Scenarios are selected for different values of SNR which are for 5dB, 10dB and 15dB shown in figure-4.6, figure-4.7 and figure-4.8 respectively.

For each case the value of p is varied from 0 to 1 which, in fact, describes the effect of impulse noise to the system. From the figures, it is clear that as the value of p is increasing, the performance of the system is getting worse. One interesting

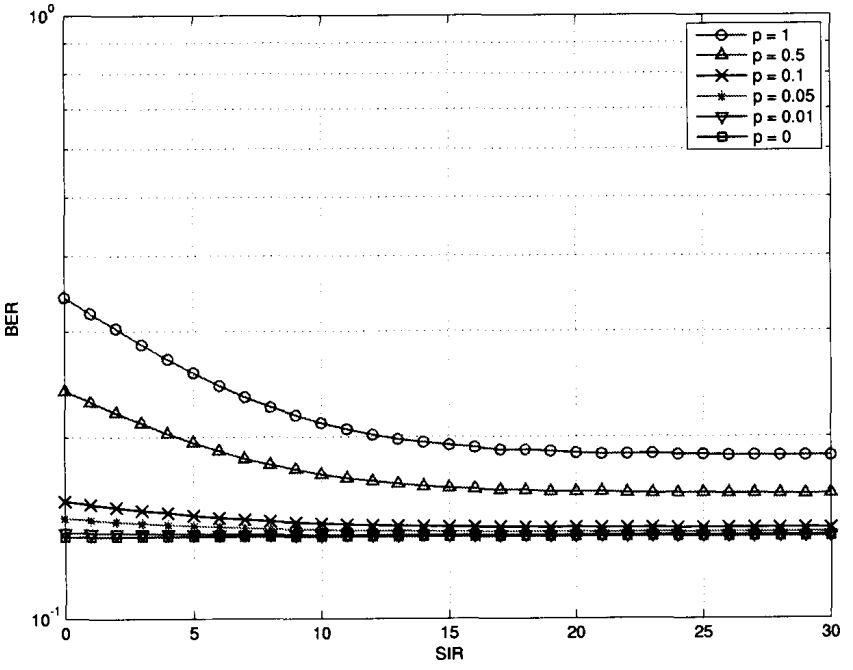

Figure 4.6: Effect of varying SIR in a co-operative communication system while SNR = 5dB

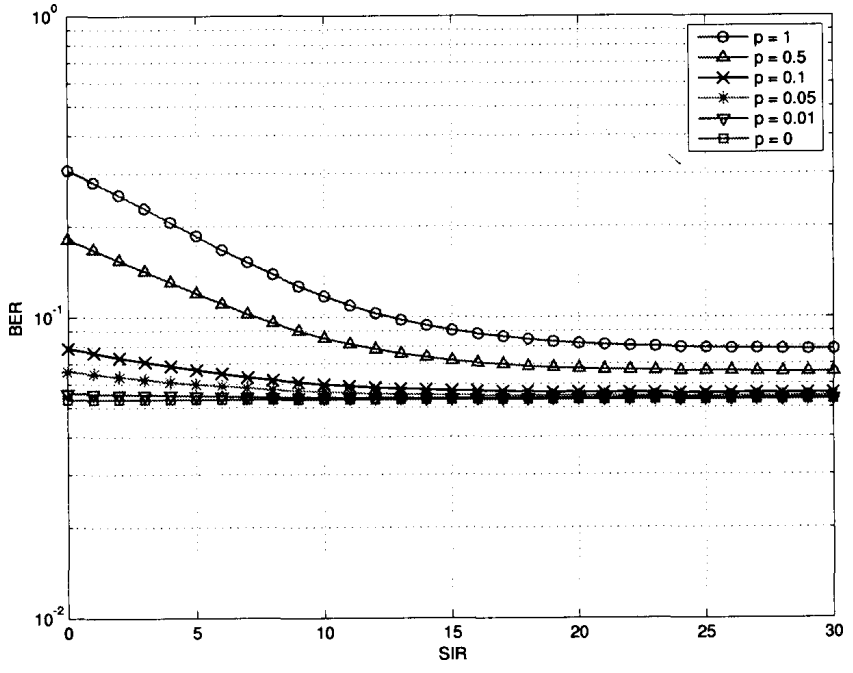

Figure 4.7: Effect of varying SIR in a co-operative communication system while SNR = 10dB

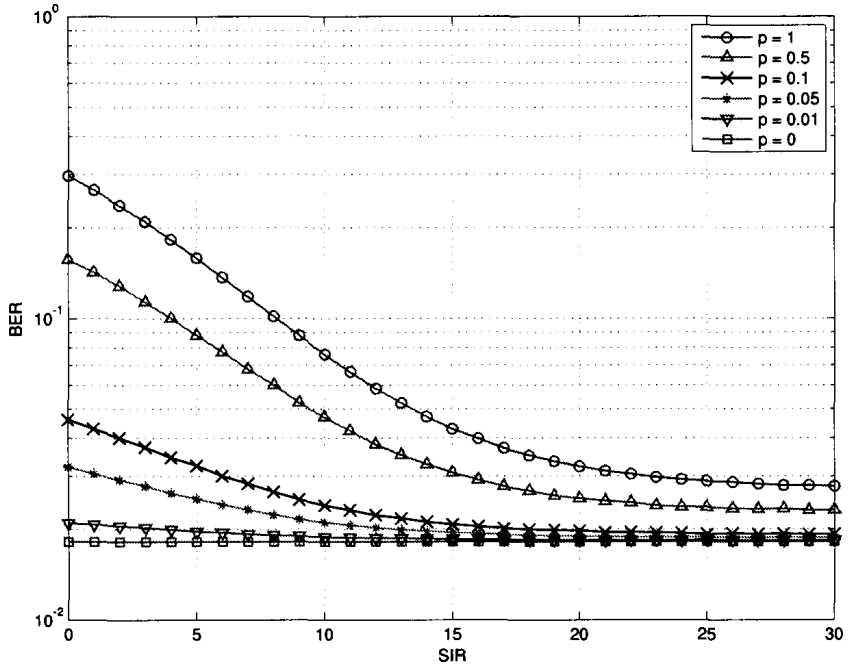

Figure 4.8: Effect of varying SIR in a co-operative communication system while SNR = 15dB

fact can be observed from here that whenever the value of p is equal to zero, the performance curve is just parallel to X-axis. When the value of p is zero, it implies that there is no impulse noise adding to the system. So in such case, there is no impact of increasing the value of SIR and the system will only experience a fixed value of AWGN which makes the curve parallel to the X-axis. Saturation effect is similar to the effect described for varying SNR.

4.2 Bi-directional Co-operative System with Diversity Technique

In this section the objective is to analyze the system performance for bi-directional relay system using multiple antennas at the source nodes while single antenna at the relay node. For simplistic analysis, it is considered that there are two antennas at

each of the source nodes. Alamouti's space time code [2] is used at the source nodes to achieve transmit diversity.

4.2.1 System Model

Throughout the bi-directional co-operative communication system, Binary Phase Shift Keying (BPSK) modulation scheme is considered. The system model is shown in the figure-4.9 where S_1 and S_2 denote two source nodes and R denotes the relay node.

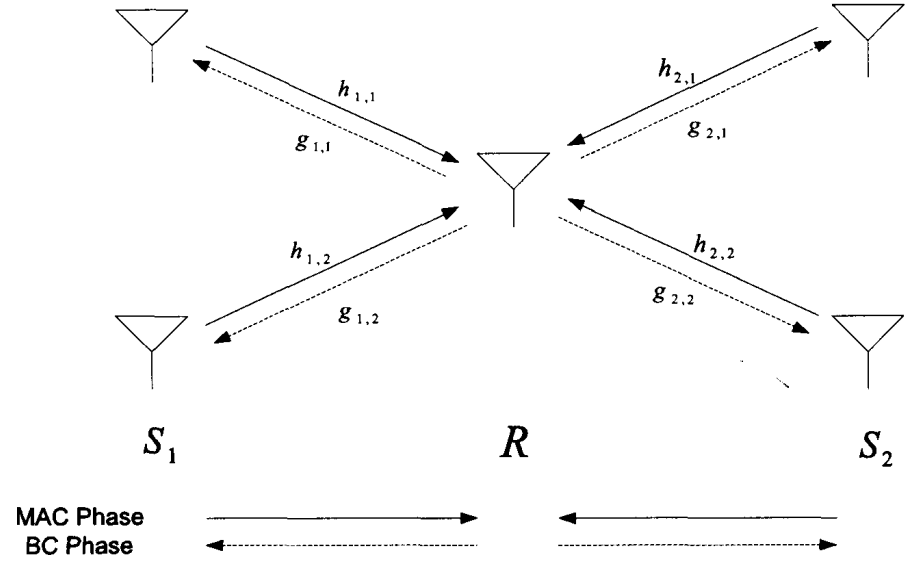

Figure 4.9: System Model of Bi-directional Co-operative Communication System

It is assumed that the channel state condition does not change during two consecutive time slots in both MAC and BC phases. Let us consider i, j and k denote the indices of antennas, time slots and source nodes respectively. As mentioned earlier, Alamouti's space time coding is used at the source node. During MAC phase, information sent by S_1 and S_2 node are $\mathbf{U}$ and $\mathbf{V}$ as follows

$$\mathbf{U} = \begin{bmatrix} u_1 & -u_2^* \\ u_2 & u_1^* \end{bmatrix} \tag{4.4}$$

$$\mathbf{V} = \begin{bmatrix} v_1 & -v_2^* \\ v_2 & v_1^* \end{bmatrix} \tag{4.5}$$

The received signal at relay node is

$$\mathbf{r}^T = \sqrt{\frac{E_1}{2}}\mathbf{h}_1^T\mathbf{U} + \sqrt{\frac{E_1}{2}}\mathbf{h}_2^T\mathbf{V} + \mathbf{w}^T \tag{4.6}$$

where $\mathbf{h}_k = \begin{bmatrix} h_{k,1} & h_{k,2} \end{bmatrix}^T$, $k = 1, 2$ is the channel condition of kth channel, E_k is transmit power at S_k and $\mathbf{w} \sim \mathcal{CN}(0, \sigma_R^2\mathbf{I}_2)$ is AWGN at relay Node R. Let us assume that XORed-like version of $(u_i, v_i), i = 1, 2$ be

$$z_i = f(u_i, v_i) = \ell^{-1}((\ell(u_i) + \ell(v_i)) \pmod M) \tag{4.7}$$

where $\ell(x) \in \left\{0, 1, ..., M-1\right\}$ is the label index of x where M is constellation size. Let us assume that the channel state information (CSI) is perfectly known at the relay node. Hence z_i can be detected as

$$\hat{z}_i = \arg\max_{z \in M} \sum_{(\mathbf{U},\mathbf{V}):f(u_i,v_i)=z} \exp(-T(\mathbf{U}, \mathbf{V})) \tag{4.8}$$

where $T(\mathbf{U}, \mathbf{V}) = \left\| \frac{\mathbf{r}^T}{\sigma_R} - \sqrt{\frac{\bar{\gamma}_1}{2}}\mathbf{h}_1^T\mathbf{U} - \sqrt{\frac{\bar{\gamma}_2}{2}}\mathbf{h}_2^T\mathbf{V} \right\|^2$ and $\bar{\gamma}_k = E_k/\sigma_R^2$ is the signal to noise ratio at relay node from k source node to relay. Since it is considered that fading channels are totally independent of each other, there is zero probability

that channels will have any relationships with each other. Hence the solution for equation-4.8 should be uniquely decided.

In time slot j of the Broadcast phase, S_k receives:

$$\mathbf{y}_{k,j} = \sqrt{E_R}\mathbf{g}_k\hat{z}_j + \mathbf{n}_{k,j}, \quad j = 1, 2 \tag{4.9}$$

where E_R is the transmit power at relay node R, $\mathbf{g}_k = \begin{bmatrix} g_{k,1} & g_{k,2} \end{bmatrix}^T$ is the channel state condition of the channel from relay node to k node and $\mathbf{n}_{k,j} \sim \mathcal{CN}(0, \sigma_k^2\mathbf{I}_2)$ is Gaussian Noise at S_k. Now S_k detects $\hat{z}_j$ as

$$\tilde{z}_{k,j} = \arg\min_{z \in M} \left\| \frac{\mathbf{y}_k, j}{\sigma_k} - \sqrt{\bar{\gamma}_{k+2}}\mathbf{g}_k z \right\|^2 \tag{4.10}$$

where $\bar{\gamma}_{k+2} = E_R/\sigma_k^2$ is the SNR at the node k. Each source node then finally detects the information sent by the peer source node as

$$\begin{aligned} v_i &= \ell^{-1}((\ell(\tilde{z}_{1,j}) - \ell(u_i)) \pmod M) \\ u_i &= \ell^{-1}((\ell(\tilde{z}_{2,j}) - \ell(v_i)) \pmod M) \end{aligned} \tag{4.11}$$

where $i = j \in \{1, 2\}$

4.2.2 Error Probability Analysis

In our system model, $\mathbf{g}_k$ can be assumed independent or identical to $\mathbf{h}_k$. Basically it depends upon the channels between S_k and R. For simplicity let us assume that $g_k = h_k$, $k = 1, 2$. It is also assumed that $h_{k,i}, k = 1, 2; i = 1, 2$ are independent and $h_{k,i} \sim \mathcal{CN}(0, 1)$ which actually indicates that they are Rayleigh Fading Channels.

Let P_{mac} denotes the Symbol Error Probability (SEP) in MAC phase and can be expressed by (for h_1 and h_2)

$$P_{mac} \triangleq \frac{1}{2}\Big[\Pr\{\hat{z}_1 \neq f(u_1, v_1)|(\mathbf{U}, \mathbf{V}), \mathbf{h}_1, \mathbf{h}_2\} + \Pr\{\hat{z}_2 \neq f(u_2, v_2)|(\mathbf{U}, \mathbf{V}), \mathbf{h}_1, \mathbf{h}_2\}\Big] \tag{4.12}$$

Let us assume that $P_{bc,k}$ denotes the SEP during BC phase at S_k (for h_k)

$$P_{bc,k} \triangleq \frac{1}{2}\sum_{j=1}^{2}\Pr\{\tilde{z}_{k,j} \neq \tilde{z}_j|\tilde{z}_j, \mathbf{h}_k\} \tag{4.13}$$

If the system had one way transmission and if there is only one error in one phase, receiver could not be able to correct the error. If both phases have errors, in that case the probability of correct detection will be $1/(M-1)$ [45]. Hence end-to-end SEP can be calculated as follows

$$P_{EtoE} = P_{mac} + \frac{1}{2}\sum_{k=1}^{2} P_{bc,k} - \frac{M}{M-1}P_{mac}\sum_{k=1}^{2} P_{bc,k} \tag{4.14}$$

The above expression is attained by the average of two way transmissions. Now the average end-to-end SEP can be obtained by

$$\bar{P}_{EtoE} = \mathbb{E}[P_{EtoE}] \tag{4.15}$$

where expectation is taken with respect to $(\mathbf{h}_1, \mathbf{h}_2)$

The purpose is now to derive the upper and lower limits. For BPSK, $P_{bc,k}$ can be expressed by

$$P_{bc,k} = Q\left(\sqrt{2\bar{\gamma}_{k+2}||\mathbf{h}_k||^2}\right) \tag{4.16}$$

where $Q(\cdot)$ is the Q-function [46].

During the MAC phase, Alamouti codewords are $\mathbf{U} = [\mathbf{U}_1, \mathbf{U}_2, \mathbf{U}_3, \mathbf{U}_4]$ and $\mathbf{V} = [\mathbf{V}_1, \mathbf{V}_2, \mathbf{V}_3, \mathbf{V}_4]$, where

$$\mathbf{U}_1 = \mathbf{V}_1 = \begin{bmatrix} 1 & -1 \\ 1 & 1 \end{bmatrix}$$

$$\mathbf{U}_2 = \mathbf{V}_2 = \begin{bmatrix} 1 & 1 \\ -1 & 1 \end{bmatrix}$$

$$\mathbf{U}_3 = \mathbf{V}_3 = \begin{bmatrix} -1 & 1 \\ -1 & -1 \end{bmatrix}$$

$$\mathbf{U}_4 = \mathbf{V}_4 = \begin{bmatrix} -1 & -1 \\ 1 & -1 \end{bmatrix}$$

The detection region for the above mentioned alphabets can not be specified easily [45]. Hence it is wise to derive the upper and lower limit of P_{mac}. Moreover, it is difficult to analyze the SEP for the ML detection rule in equation-4.8 since that is a sum of exponential functions. Let us modify the detection rule based on max-log approximation which is given by

$$\hat{z}_i = \arg \min_{z \in \{-1,1\}} \min_{(\mathbf{U},\mathbf{V}):u_i v_i = z} T(\mathbf{U}, \mathbf{V}) \tag{4.17}$$

It is now required to derive the upper and lower limit for P_{mac} which will be discussed in the next subsection.

4.2.2.1 Derivation of Upper and Lower limits for MAC phase

Without loss of generality, let us assume that $(\mathbf{U}_1, \mathbf{V}_1)$ is sent So real XORed-like symbols are $z_1 = z_2 = 1$. Let

$$T_1 = \min_{(\mathbf{U},\mathbf{V}):u_1 v_1 = 1} T(\mathbf{U}, \mathbf{V}); \qquad (\mathbf{U}, \mathbf{V}) \neq ((\mathbf{U}_1, \mathbf{V}_1) \tag{4.18}$$

$$T_2 = \min_{(\mathbf{U},\mathbf{V}):u_1 v_1 = -1} T(\mathbf{U}, \mathbf{V}) \tag{4.19}$$

Let us consider the error probability for z_1 , it can be written as [45]

$$\begin{aligned}
&\Pr\{\hat{z}_1 = -1 | (\mathbf{U}_1, \mathbf{V}_1), \mathbf{h}_1, \mathbf{h}_2\} \\
&= \Pr\{\min(T(\mathbf{U}_1, \mathbf{V}_1), T_1) > T_2 | (\mathbf{U}_1, \mathbf{V}_1)\} \\
&= \Pr\{(T_1 \geq T(\mathbf{U}_1, \mathbf{V}_1)) \& (T(\mathbf{U}_1, \mathbf{V}_1) > T_2) | (\mathbf{U}_1, \mathbf{V}_1)\} \\
&\quad + \Pr\{(T(\mathbf{U}_1, \mathbf{V}_1) > T_1) \& (T_1 > T_2) | (\mathbf{U}_1, \mathbf{V}_1)\} \\
&\leq \Pr\{T(\mathbf{U}_1, \mathbf{V}_1) > T_2 | (\mathbf{U}_1, \mathbf{V}_1)\} \\
&\quad + \Pr\{T(\mathbf{U}_1, \mathbf{V}_1) > T_1 | (\mathbf{U}_1, \mathbf{V}_1)\} \\
&\leq \sum_{(m,n) \neq (1,1)} \Pr\{T(\mathbf{U}_1, \mathbf{V}_1) > T(\mathbf{U}_m, \mathbf{V}_n) | (\mathbf{U}_1, \mathbf{V}_1)\} \\
&= \sum_{(m,n \neq (1,1))} P_{PEP,m,n}
\end{aligned}$$

where

$$P_{PEP,m,n} \triangleq Q(\mathbf{q}_{m,n}) \qquad \text{with}$$

$$\mathbf{q}_{m,n} \triangleq ||\sqrt{\frac{\bar{\gamma}_1}{4}}\mathbf{h}_1^T(\mathbf{U}_1 - \mathbf{U}_m) + \sqrt{\frac{\bar{\gamma}_2}{4}}\mathbf{h}_2^T(\mathbf{V}_1 - \mathbf{V}_m)||, \qquad 1 \leq m, n \leq 4$$

Here m and n are the indices for the codewords. Same derivation can be done for z_2 and then upper bound for P_{mac} can be achieved.

To derive the lower bound, let us assume that the relay node is able to detect $\mathbf{U}$ if $\bar{\gamma}_1||\mathbf{h}_1||^2 > \bar{\gamma}_2||\mathbf{h}_2||^2$ or $\mathbf{V}$ if $\bar{\gamma}_2||\mathbf{h}_2||^2 > \bar{\gamma}_1||\mathbf{h}_1||^2$. If the relay can detect this, the system performance would be better than the system described in Section-4.2.1. If $\mathbf{U}$ is known, $P_{mac} \geq Q\left(\sqrt{\bar{\gamma}_2||\mathbf{h}_2||^2}\right)$ and if $\mathbf{V}$ is known, $P_{mac} \geq Q\left(\sqrt{\bar{\gamma}_1||\mathbf{h}_1||^2}\right)$

Hence lower bounds on P_{mac} can be written as

$$P_{mac}^L \triangleq Q\left(\sqrt{\min\left(\bar{\gamma}_1||\mathbf{h}_1||^2, \bar{\gamma}_2||\mathbf{h}_2||^2\right)}\right) \tag{4.20}$$

4.2.2.2 Upper and Lower bounds for End-to-End Error Probability

Now the objective is to calculate the upper and lower limits of End-to-End error probability. Once upper and lower bounds are determined, it can be used to justify the simulation.

From Section-4.2.2.1 and Equation-4.14, it can be written

$$\begin{aligned} &\max\left(\mathbb{E}[P_{mac}^L], \frac{1}{2}\sum_{k=1}^{2}\mathbb{E}[P_{bc,k}]\right) \leq \bar{P}_{EtoE} \\ &\leq \mathbb{E}[P_{mac}^U] + \frac{1}{2}\sum_{k=1}^{2}\mathbb{E}[P_{bc,k}] \end{aligned} \tag{4.21}$$

It can be observed that $||\mathbf{h}_k||^2$ is chi-square distributed with 4 degrees of freedom. Hence

$$\mathbb{E}[P_{bc,k}] = \phi(2, \bar{\gamma}_{k+2}) \tag{4.22}$$

where

$$\phi(L,x) \triangleq \left[\frac{1-\mu(x)}{2}\right]^L \sum_{l=0}^{L-1} \binom{L-1+l}{l} \left[\frac{1+\mu(x)}{2}\right]^l \tag{4.23}$$

with $\mu(x) \triangleq \sqrt{\frac{x}{1+x}}$ [46]

Now since $(\mathbf{U}_1 - \mathbf{U}_m)$ and $(\mathbf{V}_1 - \mathbf{V}_m)$ are both orthogonal matrices, it can be said

$$\mathbf{q}_{m,n} = \sqrt{\bar{\alpha}_{m,n}}\mathbf{a}_{m,n}^T \tag{4.24}$$

where $\mathbf{a}_{m,n} = [a_{m,n,1}, a_{m,n,2}]^T \sim \mathcal{CN}(0, \mathbf{I}_2)$. The value of $\bar{\alpha}_{m,n}$ can be found from the table below (Table-4.1) [45]

Table 4.1: Values of $\bar{\alpha}_{m,n}$

m/n	1	2	3	4
1		$\bar{\gamma}_2$	$2\bar{\gamma}_2$	$\bar{\gamma}_2$
2	$\bar{\gamma}_1$	$\bar{\gamma}_1 + \bar{\gamma}_2$	$\bar{\gamma}_1 + 2\bar{\gamma}_2$	$\bar{\gamma}_1 + \bar{\gamma}_2$
3	$2\bar{\gamma}_1$	$2\bar{\gamma}_1 + \bar{\gamma}_2$	$2\bar{\gamma}_1 + 2\bar{\gamma}_2$	$2\bar{\gamma}_1 + \bar{\gamma}_2$
4	$\bar{\gamma}_1$	$\bar{\gamma}_1 + \bar{\gamma}_2$	$\bar{\gamma}_1 + 2\bar{\gamma}_2$	$\bar{\gamma}_1 + \bar{\gamma}_2$

The average PEP is then given by

$$\mathbb{E}[P_{PEP,m,n}] = \phi\left(2, \frac{\bar{\alpha}_{m,n}}{2}\right) \tag{4.25}$$

From Eqn-4.25 the upper bound of $\bar{P}_{EtoE}$ can be obtained as

$$\bar{P}_{EtoE}^{U} \triangleq \frac{1}{2}\phi(2,\bar{\gamma}_3) + \phi(2,\bar{\gamma}_4) + \sum_{\substack{1 \le m,n \le 4 \\ (m,n) \neq (1,1)}} \phi\big(2, \frac{\bar{\alpha}_{m,n}}{2}\big) \tag{4.26}$$

To determine lower bound of $\bar{P}_{EtoE}$, it is required to calculate $\mathbb{E}[P_{mac}^{L}]$. Let us assume,

$$\gamma_k = \bar{\gamma}_k ||\mathbf{h}_k||^2 , \qquad k = 1, 2$$
$$\beta = \min(\gamma_1, \gamma_2)$$

Here γ_k has a Cumulative Distribution Function (CDF) as

$$F_{\gamma k}(\xi) = 1 - e^{-\frac{\xi}{\bar{\gamma}_k}} - \frac{\xi}{\bar{\gamma}_k} e^{-\frac{\xi}{\bar{\gamma}_k}}$$

Hence the Probability Density Function (PDF) of β is

$$f_{\beta}(\xi) = c_1 \xi e^{-\frac{\xi}{\bar{\gamma}_k}} + \frac{c_2}{2\bar{\gamma}} \xi^2 e^{-\frac{\xi}{\bar{\gamma}_k}}$$

Therefore, we will have

$$\mathbb{E}[P_{mac}^{L}] = c_1 \bar{\gamma}^2 \phi\big(2, \frac{\bar{\gamma}}{2}\big) + c_2 \bar{\gamma}^2 \phi\big(3, \frac{\bar{\gamma}}{2}\big) \tag{4.27}$$

where

$$c_1 \triangleq \frac{1}{\bar{\gamma}_1^2} + \frac{1}{\bar{\gamma}_2^2}$$

$$c_2 \triangleq \frac{2}{\bar{\gamma}_1 \bar{\gamma}_1}$$

$$\bar{\gamma} \triangleq \frac{\bar{\gamma}_1 \bar{\gamma}_2}{\bar{\gamma}_1 + \bar{\gamma}_2}$$

If we combine the derivation of $\mathbb{E}[P_{mac}^{L}]$, the lower bound on $\bar{P}_{EtoE}$ can be calculated as

$$\bar{P}_{EtoE}^{L} \triangleq \max\left\{ c_1 \bar{\gamma}^2 \phi\left(2, \frac{\bar{\gamma}}{2}\right) + c_2 \bar{\gamma}^2 \phi\left(3, \frac{\bar{\gamma}}{2}\right), \right. \\ \left. \frac{1}{2}\phi(2, \bar{\gamma}_3) + \phi(2, \bar{\gamma}_4) \right\} \tag{4.28}$$

The derived upper and lower limit for error probability can now be used to justify the simulation of the bi-directional co-operative system.

4.2.3 Simulation and Results

For simulation our concern is mainly on three systems: A. the co-operative system described in Section-4.2.1, B. the co-operative system with single antenna at all node, C. Almouti's scheme with 2 × 2 MIMO system without any relay. Total transmit power is kept constant for each of the systems to compare them fairly. Since System-C does not have any relay, the distance between Tx and Rx is kept twice in System-C than the distance between Tx and relay or Rx and relay in System-A or Sytem-B. Noise variances are kept similar for all system. From the figure-4.10, it is certain the co-operative system described by Equation-4.8 and Equation-4.17 show almost similar performance. They are residing between the upper and lower limit of P_{EtoE} of the system. It indicates the derivation of P_{EtoE} can predict the error probability successfully. It is also obvious from the figure that system-A performs better than system-B since diversity technique is applied at system-A. System-A even performs

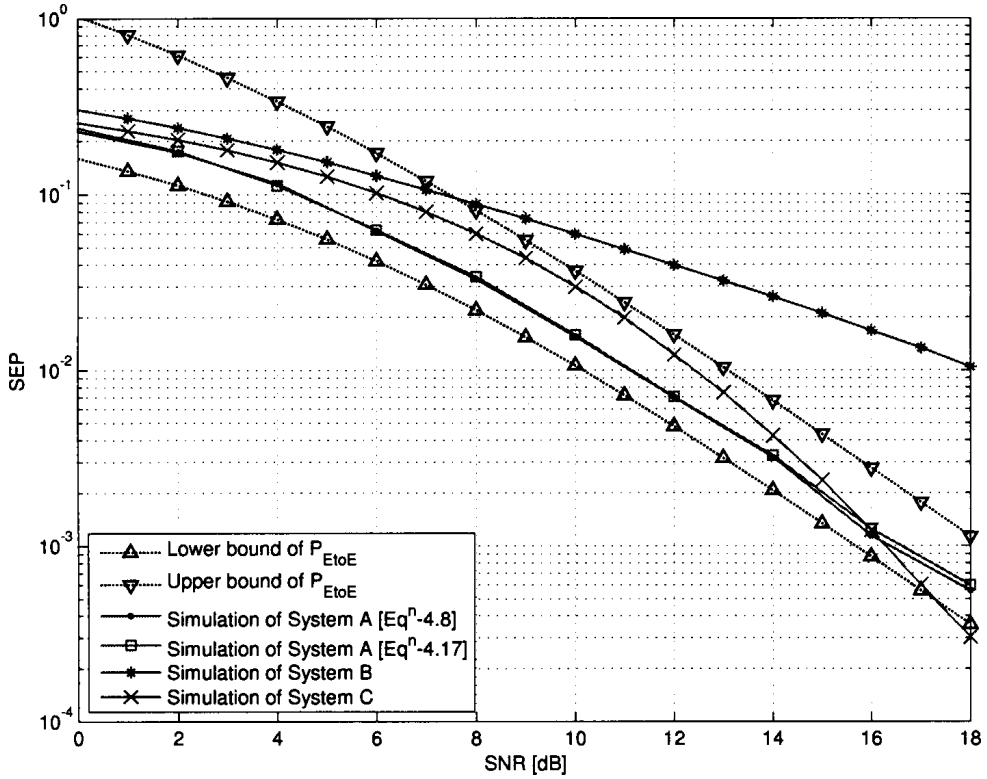

Figure 4.10: Performance comparison of different systems (with and without relay)

better than System-C as well when the SNR is low. At high SNR, the scenario flips though.

4.3 Conclusion

In this chapter, two branches of co-operative communication system have been analyzed. At first relay system was analyzed under Impulsive Noise environment. As expected the performance deteriorates when there is dense impulse noise in the system. It was investigated by varying different parameters of the system. Secondly performance was observed when diversity technique is implemented at the source nodes in relay communication system. Theoretically the error probability was derived for such system. Later simulation was also done with same configuration. It

was found that the simulated result resided between the theoretical lower and upper limit of the probability of error.

Chapter 5

Conclusion

In this thesis, it is tried to investigate some important and promising fields in wireless communication. At first diversity technique, more specifically space diversity, is explored comprehensively with its ins and outs. There were some assumptions made while implementing diversity technique in wireless communication system. For example, it is considered that channel does not change in two consecutive time slots, channel condition is perfectly known at the reception side etc. However these situation might not be the case in practical. Practically it is difficult to have scenario such that channel does not change in two time slots. Moreover to estimate the channel perfectly, pilot symbols are sent along with the original signal. When the channel fades very quickly, it will not be possible to determine the channel with the aid of pilot symbol since they are normally sent after some time period. Such practical scenarios are considered while implementing Alamouti's scheme. Then theoretically it was determined how probability of error varies along with the data SNR and pilot SNR. Simulation was also done to show the performance of such system. Moreover other parameters like angle of arrival, doppler spread etc. which are useful to make the system more practical are also considered. Performances were also analyzed for the system while considering such important factors.

Performance was evaluated for another hot cake in wireless research arena, namely, co-operative communication system. At first system performance was evaluated for typical co-operative communication system. Later it was implemented for

an industrial application where impulse noise comes into the picture. System performance was evaluated in such environment varying SNR keeping SINR fixed and vice versa. While one parameter remained fixed, simulation was also done for different values of that parameter and then result was analyzed. From the simulation result it was found that impulse noise can change the overall performance severely depending upon the intensity of impulse noise. In next part of the thesis, co-operative communication system is blended with the diversity technique. This is also a new research area to work with. When diversity technique is merged with relay communication system, advantages can be attained from both. Theoretically the system performance is evaluated for such system by deriving upper and lower limits of probability of error. Later system performance was determined by simulating the whole system. The simulated results were found according to the expression obtained from the theoretical analysis.

In future this work can be extended for different modulation scheme. Experimental data can be collected from an industrial application and then simulation can be done to obtain exact result for that specific environment. There are also some assumptions made while combining relay system and MIMO system. Performance can be evaluated considering practical scenario as well. It can be mentioned here that publication work will be done after the thesis is completed.

References

[1] W.C.Jakes, *Microwave Mobile Communication.* New Jersey: IEEE Press, 1994.

[2] S. Alamouti, "A simple transmit diversity technique for wireless communications," *Selected Areas in Communications, IEEE Journal on*, vol. 16, pp. 1451 –1458, oct. 1998.

[3] K. J. R. Liu, A. K. Sadek, W. Su, and A. Kwasinski, *Cooperative Communications and Networking.* Cambridge University Press, 2009.

[4] S. Al-Dharrab and M. Uysal, "Cooperative diversity in the presence of impulsive noise," *Wireless Communications, IEEE Transactions on*, vol. 8, no. 9, pp. 4730 –4739, 2009.

[5] A. Abdaoui, S. Ikki, M. Ahmed, and E. Chatelet, "On the performance analysis of a mimo-relaying scheme with space time block codes," *Vehicular Technology, IEEE Transactions on*, vol. 59, no. 7, pp. 3604 –3609, 2010.

[6] A. Papoulis, *Probability, Random Variables, and Stochastic Processes.* McGraw-Hill Inc., 1991.

[7] O. C. Ibe, *Fundamentals of Applied Probability and Random Processes.* Elsevier Academic Press, 2005.

[8] H. P. Hsu, *Schaum's Outline of Theory and Problems of Probability, Random Variables, and Random Processes.* McGraw-Hill, 1997.

[9] J. A. Gubner, *Probability and Random Processes for Electrical and Computer Engineers.* Cambridge University Press, 2006.

[10] T. S. Rappaport, *Wireless Communications: Principles and Practice.* Prentice-Hall Inc., 2000.

[11] B. Sklar, *Digital Communications: Fundamentals and Applications.* Prentice Hall PTR, 2001.

[12] H. Jafarkhani, *Space-Time Coding: Theory and Practice.* Cambridge University Press, 2005.

[13] T. M. Duman and A. Ghrayeb, *Coding for MIMO Communication Systems.* John Wiley Sons Ltd., 2007.

[14] M. Jankiraman, *Space-Time Codes and MIMO Systems.* Artech House Inc, 2004.

[15] M. Ghosh, "Analysis of the effect of impulse noise on multicarrier and single carrier qam systems," *Communications, IEEE Transactions on*, vol. 44, pp. 145 –147, Feb. 1996.

[16] M.-S. A. Marvin K. Simon, *Digital Communication over Fading Channels.* Wiley-Interscience, 2000.

[17] J. Jootar, J. Zeidler, and J. Proakis, "Performance of alamouti space-time code in time-varying channels with noisy channel estimates," vol. 1, pp. 498 – 503 Vol. 1, mar. 2005.

[18] J. Y. Branka Vucetic, *Space-time coding.* John Wiley and Sons Inc., 2005.

[19] E. Peh, Y.-C. Liang, and Y. L. Guan, "Power control for physical-layer network coding in fading environments," in *Personal, Indoor and Mobile Radio Communications, 2008. PIMRC 2008. IEEE 19th International Symposium on*, pp. 1–5, 2008.

[20] J.-K. Zhang and W.-K. Ma, "Full diversity blind alamouti space-time block codes for unique identification of flat-fading channels," *Signal Processing, IEEE Transactions on*, vol. 57, pp. 635 –644, feb. 2009.

[21] C. W. Tan and A. Calderbank, "Multiuser detection of alamouti signals," *Communications, IEEE Transactions on*, vol. 57, pp. 2080 –2089, jul. 2009.

[22] A. Vielmon, Y. Li, and J. Barry, "Performance of alamouti transmit diversity over time-varying rayleigh-fading channels," *Wireless Communications, IEEE Transactions on*, vol. 3, pp. 1369 – 1373, sep. 2004.

[23] Y. Zhang and D. Li, "Performance of space-time transmit diversity over time-selective fading channels," vol. 1, pp. 402 – 405 Vol.1, sep. 2003.

[24] G. L. Turin, "The characteristic function of hermitian quadratic forms in complex normal variables," *Biometrika*, pp. 47: 199–201, 1960.

[25] P. V. O'Neil, *Advanced Engineering Mathematics.* Thomson tm, 6th ed., 2007.

[26] E. Biglieri, G. Caire, G. Taricco, and J. Ventura-Traveset, "Simple method for evaluating error probabilities," *Electronics Letters*, vol. 32, pp. 191 –192, feb. 1996.

[27] D. Gu and C. Leung, "Performance analysis of transmit diversity scheme with imperfect channel estimation," *Electronics Letters*, vol. 39, pp. 402 – 403, feb. 2003.

[28] A. Abdi and M. Kaveh, "A space-time correlation model for multielement antenna systems in mobile fading channels," *Selected Areas in Communications, IEEE Journal on*, vol. 20, pp. 550 –560, Apr. 2002.

[29] A. Abdi, J. Barger, and M. Kaveh, "A parametric model for the distribution of the angle of arrival and the associated correlation function and power spectrum at the mobile station," *Vehicular Technology, IEEE Transactions on*, vol. 51, pp. 425 –434, May 2002.

[30] J. Laneman and G. Wornell, "Distributed space-time-coded protocols for exploiting cooperative diversity in wireless networks," *Information Theory, IEEE Transactions on*, vol. 49, no. 10, pp. 2415 – 2425, 2003.

[31] J. Laneman, D. Tse, and G. Wornell, "Cooperative diversity in wireless networks: Efficient protocols and outage behavior," *Information Theory, IEEE Transactions on*, vol. 50, no. 12, pp. 3062 – 3080, 2004.

[32] A. Sendonaris, E. Erkip, and B. Aazhang, "User cooperation diversity-part i: System description," *Communications, IEEE Transactions on*, vol. 51, no. 11, pp. 1927 – 1938, 2003.

[33] A. Sendonaris, E. Erkip, and B. Aazhang, "User cooperation diversity-part ii: Implementation aspects and performance analysis," *Communications, IEEE Transactions on*, vol. 51, no. 11, pp. 1939 – 1948, 2003.

[34] S. Yiu, R. Schober, and L. Lampe, "Distributed space-time block coding for cooperative networks with multiple-antenna nodes," in *Computational Advances in Multi-Sensor Adaptive Processing, 2005 1st IEEE International Workshop on*, pp. 52 – 55, 2005.

[35] E. C. V. der Meulen, "Three-terminal communication channels," *Advances in Applied Probability*, vol. 3, no. 1, pp. 120–154, 1971.

[36] M. Ju and I.-M. Kim, "Error performance analysis of bpsk modulation in physical-layer network-coded bidirectional relay networks," *Communications, IEEE Transactions on*, vol. 58, pp. 2770 –2775, october 2010.

[37] P. Popovski and H. Yomo, "Wireless network coding by amplify-and-forward for bi-directional traffic flows," *Communications Letters, IEEE*, vol. 11, no. 1, pp. 16 –18, 2007.

[38] P. Popovski and H. Yomo, "The anti-packets can increase the achievable throughput of a wireless multi-hop network," in *Communications, 2006. ICC '06. IEEE International Conference on*, vol. 9, pp. 3885 –3890, 2006.

[39] S. Zhang, S. chang Liew, and P. P. Lam, "Physical-layer network coding," in *ACM Mobicom '06*, pp. 358–365, 2006.

[40] S. Katti, S. Gollakota, and D. Katabi, "Embracing wireless interference: analog network coding," *SIGCOMM Comput. Commun. Rev.*, vol. 37, pp. 397–408, August 2007.

[41] D. Middleton, "Statistical-physical models of electromagnetic interference," *Electromagnetic Compatibility, IEEE Transactions on*, vol. EMC-19, no. 3, pp. 106 –127, 1977.

[42] B. Rankov and A. Wittneben, "Spectral efficient protocols for half-duplex fading relay channels," *Selected Areas in Communications, IEEE Journal on*, vol. 25, no. 2, pp. 379 –389, 2007.

[43] S. Zhang, S. C. Liew, and L. Lu, "Physical layer network coding schemes over finite and infinite fields," in *Global Telecommunications Conference, 2008. IEEE GLOBECOM 2008. IEEE*, 30 2008.

[44] T. Cui, F. Gao, T. Ho, and A. Nallanathan, "Distributed space-time coding for two-way wireless relay networks," in *Communications, 2008. ICC '08. IEEE International Conference on*, pp. 3888 –3892, May 2008.

[45] D. To, J. Choi, and I. Kim, "Error probability analysis of bidirectional relay systems using alamouti scheme," *Communications Letters, IEEE*, vol. 14, no. 8, pp. 758 –760, 2010.

[46] J. G. Proakis, *Digital Communications.* New York: McGraw-Hill, 1995.

Appendix A
Derivation of Combining Scheme

A.1 Derivation of Combining Scheme (Tx=2, Rx=1)

First combining equation is given by

$$s_0 = h_0^* r_0 + h_1 r_1^* \tag{A.1}$$

Putting the values of r_0 and r_1

$$\begin{aligned} s_0 &= h_0^*(h_0 s_0 + h_1 s_1 + n_0) + h_1(-h_0^* s_1 + h_1^* s_0 + n_1^*) \\ &= h_0^2 s_0 + h_0^* h_1 s_1 + h_0^* n_0 - h_1 h_0^* s_1 + h_1^2 s_0 + h_1 n_1^* \\ &= s_0(h_0^2 + h_1^2) + h_0^* n_0 + h_1 n_1^* \end{aligned} \tag{A.2}$$

Second combining equation is given by

$$s_1 = h_1^* r_0 - h_0 r_1^* \tag{A.3}$$

Putting the values of r_0 and r_1

$$\begin{aligned} s_1 &= h_1^*(h_0 s_0 + h_1 s_1 + n_0) - h_0(-h_0^* s_1 + h_1^* s_0 + n_1^*) \\ &= h_1^* h_0 s_0 + h_1^2 s_1 + h_1^* n_0 + h_0^2 s_1 - h_0 h_1^* s_0 - h_0 n_1^* \\ &= s_1(h_0^2 + h_1^2) + h_1^* n_0 - h_0 n_1^* \end{aligned} \tag{A.4}$$

A.2 Derivation of Combining Scheme (Tx=2, Rx=2)

First combining equation is given by

$$s_0 = h_0^* r_0 + h_1 r_1^* + h_2^* r_2 + h_3 r_3^* \tag{A.5}$$

Putting the values of r_0 , r_1, r_2 and r_3

$$\begin{aligned} s_0 &= h_0^*(h_0 s_0 + h_1 s_1 + n_0) + h_1(-h_0^* s_1 + h_1^* s_0 + n_1^*) \\ &\quad + h_2^*(h_2 s_0 + h_3 s_1 + n_2) + h_3(-h_2^* s_1 + h_3^* s_0 + n_3^*) \\ &= h_0^2 s_0 + h_0^* h_1 s_1 + h_0^* n_0 - h_1 h_0^* s_1 + h_1^2 s_0 + h_1 n_1^* + h_2^2 s_0 \\ &\quad + h_2^* h_3 s_1 + h_2^* n_2 - h_3 h_2^* s_1 + h_3^2 s_0 + h_3 n_3^* \\ &= s_0(h_0^2 + h_1^2 + h_2^2 + h_3^2) + h_0^* n_0 + h_1 n_1^* + h_2^* n_2 + h_3 n_3^* \end{aligned} \tag{A.6}$$

Second combining equation is given by

$$s_1 = h_1^* r_0 - h_0 r_1^* + h_3^* r_2 - h_2 r_3^* \tag{A.7}$$

Putting the values of r_0 , r_1, r_2 and r_3

$$\begin{aligned} s_1 &= h_1^*(h_0 s_0 + h_1 s_1 + n_0) - h_0(-h_0^* s_1 + h_1^* s_0 + n_1^*) \\ &\quad + h_3^*(h_2 s_0 + h_3 s_1 + n_2) - h_2(-h_2^* s_1 + h_3^* s_0 + n_3^*) \\ &= h_1^* h_0 s_0 + h_1^2 s_1 + h_1^* n_0 + h_0^2 s_1 - h_0 h_1^* s_0 - h_0 n_1^* \\ &\quad + h_3^* h_2 s_0 + h_3^2 s_1 + h_3^* n_2 + h_2^2 s_1 - h_2 h_3^* s_0 - h_2 n_3^* \\ &= s_1(h_0^2 + h_1^2 + h_2^2 + h_3^2) + h_1^* n_0 - h_0 n_1^* + h_3^* n_2 - h_2 n_3^* \end{aligned} \tag{A.8}$$

Appendix B

Residues of Scaled Poles

The objective is to demonstrate the residues are invariant to the scaling of the poles. In other words, the residue of $\Phi(s)/s$ at pole p is equal to the residue $\Phi(as)/s$ at pole p/a, where a is the scaling factor. Let us consider a function $\Phi(s)/s$ such that

$$\frac{\Phi(s)}{s} = \frac{1}{s\prod_{k=1}^{2d}(\lambda_i s - 1)} = \frac{1}{s\prod_{k=1}^{2d}\lambda_i(s - 1/\lambda_i)}$$
$$= \frac{k_0^1}{s} + \frac{k_1^1}{(s-1/\lambda_1)} + \frac{k_2^1}{(s-1/\lambda_2)} + \frac{k_2^2}{(s-1/\lambda_2)^2} + \frac{k_2^3}{(s-1/\lambda_2)^3} + \cdots \quad \text{(B.1)}$$

Let us substitute $s = a\tilde{s}$. Then Eqn-B.1 becomes

$$\frac{\Phi(a\tilde{s})}{a\tilde{s}} = \frac{k_0^1}{a\tilde{s}} + \frac{k_1^1}{(a\tilde{s}-1/\lambda_1)} + \frac{k_2^1}{(a\tilde{s}-1/\lambda_2)} + \frac{k_2^2}{(a\tilde{s}-1/\lambda_2)^2} + \frac{k_2^3}{(a\tilde{s}-1/\lambda_2)^3} + \cdots \quad \text{(B.2)}$$

Multiplying both sides by a will yield

$$\frac{\Phi(a\tilde{s})}{\tilde{s}} = \frac{k_0^1}{\tilde{s}} + \frac{k_1^1}{(\tilde{s}-1/a\lambda_1)} + \frac{k_2^1}{(\tilde{s}-1/a\lambda_2)} + \frac{k_2^2/a}{(\tilde{s}-1/a\lambda_2)^2} + \frac{k_2^3/a^2}{(\tilde{s}-1/a\lambda_2)^3} + \cdots \quad \text{(B.3)}$$

From Eqn-B.3, it is clear that when we change the function from $\Phi(s)/s$ to $\Phi(as)/s$, the pole is changeed from $1/\lambda_i$ to $1/a\lambda_i$. Residues of $\Phi(as)/s$ at pole $1/a\lambda_i$

do not vary from the residues of $\Phi(s)/s$ at pole $1/\lambda_i$. Hence it can be concluded that residue is invariant to the scaling of the poles.